Government of **Western Australia**
Department of **Mines, Industry Regulation and Safety**

RECORD 2018/15

A NEW LOOK AT LAMPROPHYRES AND SANUKITOIDS, AND THEIR RELATIONSHIP TO THE BLACK FLAG GROUP AND GOLD PROSPECTIVITY

by
RH Smithies, Y Lu, CL Kirkland, KF Cassidy, DC Champion, J Sapkota, M De Paoli and L Burley

Geological Survey of Western Australia

Government of **Western Australia**
Department of **Mines, Industry Regulation and Safety**

RECORD 2018/15

A NEW LOOK AT LAMPROPHYRES AND SANUKITOIDS, AND THEIR RELATIONSHIP TO THE BLACK FLAG GROUP AND GOLD PROSPECTIVITY

by
RH Smithies, Y Lu, CL Kirkland[1], KF Cassidy[2], DC Champion[3], J Sapkota, M De Paoli and L Burley

1 Centre for Exploration Targeting (CET), Curtin Node, School of Earth and Planetary Sciences, Curtin University, Bentley WA 6845, Australia

2 Bare Rock Geological Services Pty Ltd, PO Box 1633, Fremantle WA 6959, Australia

3 Geoscience Australia, GPO Box 378, Canberra ACT 2601, Australia

PERTH 2018

Geological Survey of Western Australia

MINISTER FOR MINES AND PETROLEUM
Hon Bill Johnston MLA

DIRECTOR GENERAL, DEPARTMENT OF MINES, INDUSTRY REGULATION AND SAFETY
David Smith

EXECUTIVE DIRECTOR, GEOLOGICAL SURVEY AND RESOURCE STRATEGY
Jeff Haworth

REFERENCE
The recommended reference for this publication is:
Smithies, RH, Lu, Y, Kirkland, CL, Cassidy, KF, Champion, DC, Sapkota, J, De Paoli, M and Burley, L 2018, A new look at lamprophyres and sanukitoids, and their relationship to the Black Flag Group and gold prospectivity: Geological Survey of Western Australia, Record 2018/15, 23p.

ISBN 978-1-74168-834-4
ISSN 2204-4345

Grid references in this publication refer to the Geocentric Datum of Australia 1994 (GDA94). Locations mentioned in the text are referenced using Map Grid Australia (MGA) coordinates, Zone 50. All locations are quoted to at least the nearest 100 m.

EXPLORATION INCENTIVE SCHEME

Published 2018 by the Geological Survey of Western Australia
This Record is published in digital format (PDF) and is available online at <www.dmp.wa.gov.au/GSWApublications>.

Further details of geological products and maps produced by the Geological Survey of Western Australia are available from:
Information Centre
Department of Mines, Industry Regulation and Safety
100 Plain Street
EAST PERTH WESTERN AUSTRALIA 6004
Telephone: +61 8 9222 3459 Facsimile: +61 8 9222 3444
www.dmp.wa.gov.au/GSWApublications

Cover image: Elongate salt lake on the Yilgarn Craton — part of the Moore–Monger paleovalley — here viewed from the top of Wownaminya Hill, 20 km southeast of Yalgoo, Murchison Goldfields. Photograph by I Zibra, DMIRS

Contents

Abstract 1
Introduction 1
    Definitions and petrogenetic models 2
Sample dataset and Eastern Goldfields greenstone geochemical barcoding project 2
Analytical procedure for new samples 3
Alteration 4
Sample coverage, age and description 4
Geochemical characteristics 5
    Felsic volcanic rocks 9
    Composition variations within the Black Flag Group 11
Discussion 17
    Source regions 17
    Comparisons with regional granitic rocks 18
    A relationship with gold mineralization? 18
Conclusions 21
Acknowledgements 22
References 22

Figures

1. Location of samples within the Eastern Goldfields Superterrane (EGST) 3
2. Photos of lamprophyric rocks and enriched diorites (sanukitoids) 5
3. Location of specific rock compositional groups 6
4. Variation of selected elements for lamprophyric and associated rocks 7
5. Mantle-normalized multi-element diagrams for lamprophyric and associated rocks 8
6. Variation of Nb/Zr with $a SiO_2$ for lamprophyric and associated rocks 9
7. Variation in aP_2O_5, Sr, Th, Zr and La with $Mg^{\#}$ comparing lamprophyric and associated rocks Paringa Basalt 9
8. Variation of Cr with $aSiO_2$ for lamprophyric and associated rocks 10
9. Variation of $Mg^{\#}$ with aMgO for closely spatially associated lamprophyric and associated rocks 10
10. Variation of selected major elements, major element ratios and trace elements for all rock groups 12, 13
11. Variation of Nb with aP_2O_5 for all rock groups 14
12. Mantle-normalized multi-element diagrams for enriched and unenriched felsic rocks 14
13. Variation of La/Nb with $aSiO_2$ and with Nb for all rock groups 15
14. Photomicrographs of apatite–magnetite–biotite assemblages in the BFG 15
15. Variation of aP_2O_5 with total Fe (as $aFe_2O_3^T$), Ba, SO_3, As, $aTiO_2$ and Y 16
16. Variation in Nb with aP_2O_5 comparing the enriched and unenriched felsic rocks with Yilgarn Craton granitic rock groups 19
17. Distribution of Mafic granites 20
18. Variation in Nb with aP_2O_5 comparing the enriched and unenriched felsic rocks with Yilgarn Craton granitic rock groups 21

A new look at lamprophyres and sanukitoids, and their relationship to the Black Flag Group and gold prospectivity

by

RH Smithies, Y Lu, CL Kirkland[1], KF Cassidy[2], DC Champion[3], J Sapkota, M De Paoli and L Burley

Abstract

A significant increase in the amount of high-quality lithogeochemical data from volcanic and subvolcanic rocks of the Eastern Goldfields Superterrane (EGST) allows a robust assessment of links between lamprophyric intrusions and trace element-enriched dioritic intrusions, links between these and felsic volcanic rocks, including the Black Flag Group (BFG), and links between all of these and gold prospectivity. Enriched dioritic intrusions into greenstones, commonly found in association with lamprophyric rocks, have all the compositional hallmarks of sanukitoids (dioritic to granodioritic magmas derived from metasomatized lithospheric mantle). Contrary to most previous models, lamprophyric magmas and sanukitoids of the EGST are genetically related through amphibole fractionation; sanukitoids are not direct extracts from a lithospheric source. Together, lamprophyres and sanukitoids define a distinct low Nb, high P_2O_5 magmatic association. More than 75% of 'Mafic granites' (one of the four main granitic rock groups of the Yilgarn Craton) fall within this association. Most significantly, more that 75% of the igneous rocks forming the BFG itself also fall within this distinct 'enriched' association, i.e. most BFG rocks are volcanic equivalents of evolved sanukitoids (or Mafic granites). Smaller occurrences of similar felsic volcanic rocks lie throughout the EGST but are not as abundant or regionally extensive as 'unenriched' felsic volcanic and subvolcanic rocks. The origins of the enriched magmas can be traced back to a metasomatized lithospheric source and so the occurrence of such magmas indicates proximity to a translithospheric structure. The significance of a genetic link between lamprophyric magmas and sanukitoids, and further to more evolved dacitic (and rhyolitic) compositions of the BFG, is that protracted fractionation of wet, hornblende-bearing, lamprophyric magma involves exsolving enormous volumes of relatively oxidized fluids, which are subsequently channelled along translithospheric pathways. Even if such fluids are not initially intrinsically gold rich, they likely scavenge a significant metal cargo as they ascend through the crustal greenstone sequences. Additionally, even if such a process seldom produced primary gold mineralization, it may have represented a critical enrichment process along long-lived fluid pathways.

KEYWORDS: Archean, gold, lamprophyre, sanukitoid, Yilgarn Craton

Introduction

The relative contributions that crustal and magmatic sources have made to the Archean gold endowment of the Eastern Goldfields Superterrane (EGST) of the Yilgarn Craton have been debated for several decades without any ensuing, clear, consensus. From an empirical perspective, however, several specific intrusive magma types have been directly linked to gold mineralization. These include lamprophyres and sanukitoids (e.g. Rock and Groves, 1988a,b; Rock et al., 1989). Furthermore, recent work by Witt et al. (2013, 2015) and Witt (2016) has established a clear, statistically valid basis for these empirical observations.

The capacity of Phanerozoic mantle-metasomatic processes to greatly enrich metals in the mantle-lithospheric sources for later magmas is well documented (e.g. Lorand et al., 1989; Hronsky et al., 2012), but the proxies of such intrinsic source enrichments [e.g. mantle-like platinum group elements/gold (PGE/Au) ratios] are clear but are not evident in many Archean lamprophyres or sanukitoids (e.g. Taylor et al., 1994). One obvious and long-recognized connection between these intrusions, and between them and gold deposits, is that they typically occur within, or along, regional-scale shear zones (e.g. Perring et al., 1989). Hence, a common belief is that the intrusions and gold mineralization simply follow the same structures, which mark potential sites of significant fluid circulation. Views that magmatism simply supplied the heat, or was itself an expression of the heat, required to circulate gold-bearing fluids are difficult to disprove.

The Eastern Goldfields greenstone geochemical barcoding project is an initiative under the Exploration Incentive Scheme (EIS) that aims to geochemically characterize greenstone stratigraphy throughout the EGST. One of the substantial potential benefits to arise from the ongoing accumulation of extensive geochemical datasets is that

1 Centre for Exploration Targeting (CET), Curtin Node, School of Earth and Planetary Sciences, Curtin University, Bentley WA 6845

2 Bare Rock Geological Services Pty Ltd, PO Box 1633, Fremantle WA 6959

3 Geoscience Australia, GPO Box 378, Canberra ACT 2601

previously cryptic geochemical trends may become more obvious, and hence, their significance appraised. In this contribution, we look at new data for lamprophyric magmas, sanukitoids and high-Mg andesitic and dacitic volcanic rocks from throughout the EGST. We reassess potential links that these magmas may have with each other, with other regional felsic magmatic units, and with gold mineralization.

Definitions and petrogenetic models

The following descriptions provide useful definitions.

Lamprophyre: a highly variable group of low-volume (dykes, plugs etc.), mafic to ultramafic, intrusive rocks characterized by alkali and volatile-rich compositions and, at the subvolcanic level where they are typically recognized, biotite and/or amphibole macrocrysts (e.g. Rock and Groves, 1988a,b; Rock et al., 1989). In many Archean terranes, the close spatial and temporal link between gold mineralization and lamprophyres is specifically with 'calc-alkaline' lamprophyres. On mantle-normalized incompatible trace-element diagrams, calc-alkaline lamprophyres have highly fractionated rare earth element (REE) patterns (strongly elevated light rare earth element [LREE] concentrations) strongly elevated large ion lithophile element (LILE; Sr, Ba, Rb, Pb) concentrations but significant relative depletions (i.e. negative anomalies) in high field strength elements (HFSE: Nb, Ta, Zr, Hf, Ti). The $Mg^{\#}$ [$Mg^{\#}$ = mol Mg/(Mg+total Fe) with all Fe as Fe^{2+}] ranges to high values (i.e. >60) reflecting equilibration with mantle peridotite, and Cr and Ni concentrations are correspondingly high. Many Archean calc-alkaline lamprophyres are dominantly hornblende–porphyritic (hornblende>biotite) and strongly resemble the Caledonian 'appinites' of western Scotland (e.g. Fowler and Henney, 1996).

Calc-alkaline lamprophyres are generally thought to reflect low- to moderate-degree partial melts of metasomatically enriched mantle (peridotite), and in modern tectonic settings this is typically in continental convergent margin settings where mantle upwelling leads to melting of earlier subduction-metasomatized mantle wedge.

Archean sanukitoid series: a range of typically medium-grained, intrusive, hornblende- (± clinpyroxene-) bearing monzodioritic, dioritic to granodioritic rocks characterized by high $Mg^{\#}$ and elevated concentrations of Ni, Cr and LILE. An Archean sanukitoid series should include genetic members that, at 60wt% SiO_2, have $Mg^{\#}$ of at least 60, Cr and Ni concentrations each >100 ppm and Sr and Ba concentrations each >1000 ppm (e.g. Shirey and Hanson, 1984; Stern et al., 1989; Smithies and Champion, 2000; Martin et al., 2005). Volcanic equivalents are high-Mg andesite and low-SiO_2 adakite (e.g. Martin et al., 2005).

As with lamprophyres, the paradox with sanukitoids is that compositional features strongly implicating a peridotitic source (i.e. high $Mg^{\#}$, Cr and Ni) co-exist with strong enrichments in 'crustal' components (e.g. LILE, Th, U etc.). Thus, Archean sanukitoid is generally thought to reflect low-degree partial melts of mantle (peridotite) previously metasomatized through addition of a slab-melt component (Martin et al., 2005). Like lamprophyre and shoshonite, their petrogenesis has been linked to post-subduction destabilization of metasomatized mantle lithosphere, although they are not believed to have any direct genetic relationship (e.g. through fractionation or crustal contamination) to contemporaneous mafic or ultramafic magmatism — including the commonly temporally and spatially associated lamprophyric magmas. This potentially gives them a unique petrological status as the only felsic magmas believed to be directly extracted from a mantle source (Shirey and Hanson, 1984).

From the perspective of mineral systems, both lamprophyres and Archean sanukitoids derive from mantle sources that have been fundamentally metasomatized by trace-element rich (possibly including gold; e.g. Lorand et al., 1989) fluids or melts, are inherently hydrous (H_2O and CO_2) and relatively oxidized magmas (e.g. Rock and Groves, 1988a,b; Rock et al., 1989), with a capacity to exsolve large volumes of potentially metal-rich fluids as they fractionate or crystallize. Additionally, their very presence in outcrop identifies a translithospheric structure.

Sample dataset and Eastern Goldfields greenstone geochemical barcoding project

The geochemical dataset used in this study is an extract from the larger dataset currently being accumulated as part of the Eastern Goldfields greenstone geochemical barcoding project. Currently the barcoding project has added over 2450 new, high-quality, whole-rock major and trace-element analyses, representing a 50% increase in the amount of whole-rock geochemical data available to the public. The new dataset includes outcrop samples but is dominated by samples from >130 diamond drillcores (to date), many of these obtained through the EIS Co-funded Drilling program. Diamond drillcore samples are from a combination of stratigraphic and exploration drillholes at varying distances from exploration and mining targets. In each case, they represent the least-altered and most homogeneous material available. The full dataset will be released as part of the Geological Survey of Western Australia's (GSWA) Eastern Goldfields GIS 2019 update and will be further updated with each subsequent release of the GIS package.

The dataset used in this work initially comprised 845 analyses. This was reduced to 691 after filtering for alteration (see more information following). These 691 'least-altered' samples, include 58 analyses already published in the Western Australian Geochemistry database (WACHEM; http://geochem.dmp.wa.gov.au/geochem/), 490 samples collected or re-analysed specifically for the Eastern Goldfields greenstone geochemical barcoding project, with the remainder from various published sources. Of the 691 'least-altered' samples, 462 have been interpreted from drillcore or outcrop to be volcanic or volcaniclastic in origin, 146 of which were identified as components of the Black Flag Group (BFG), from the region broadly between Menzies and Kambalda. The remaining 316 'least-altered' volcanic or volcaniclastic samples are from elsewhere within the EGST. There are

229 analyses from various subvolcanic dykes, sills and plugs intruded into the greenstone stratigraphy and that typically comprise feldspar ± hornblende–porphyritic rocks. The petrography of the samples is not described here, but the sample material, including metamorphic assemblages, is typical of that described elsewhere as the least-altered examples of the regional greenstone lithology (e.g. Morris, 1993, 1998; Taylor et al., 1994; Morris and Witt, 1997; Morris and Kirkland, 2014; Tripp, 2013).

The study dataset has a significant bias to the Menzies–Kambalda portion of the Kalgoorlie Terrane (Fig. 1), primarily because this was the region selected for the initial phase of the Eastern Goldfields greenstone geochemical barcoding project. Elsewhere throughout the EGST, the coverage of data is significantly reduced, particularly away from regions of known mineralization. Nonetheless, there is little reason to suggest that the interpretations and conclusions drawn from this study are not regionally valid.

Analytical procedure for new samples

Samples collected under the Eastern Goldfields greenstone geochemical barcoding project were analysed at Bureau Veritas (BV) Minerals, in Canning Vale, Perth, Western Australia. Samples were visually inspected and any weathering or vein material removed. Each sample was crushed either in-house (GSWA) or by BV Minerals in a plate jaw crusher and low-Cr steel mill to produce a pulp with a nominal particle size of 90% <75 µm. A representative pulp aliquot was analysed for 13 elements as major components, loss on ignition (LOI), and 54 elements as trace elements (ppm or ppb). Major elements were determined by X-ray fluorescence (XRF) spectrometry on a fused glass disk. A fragment of each disk was then laser-ablated and analysed for 51 of the 54 minor trace elements by laser ablation inductively coupled plasma mass spectrometry (LA-ICP-MS). Gold, Pd and Pt were analysed on a separate pulp aliquot by lead collection fire assay and ICP-MS. Data quality was monitored by 'blind' insertion of sample duplicates (i.e. a second pulp aliquot), internal reference materials, and the certified reference material OREAS 24b. BV Minerals also included duplicate samples, certified reference materials (including OREAS 24b), and blanks. An assessment of accuracy and precision was made using data for 17 analyses of OREAS 24b, determined during the analysis of greenstones. For analytes where the concentration is at least 10 times the lower level of detection, a measure of accuracy is provided by the agreement between the average determined value and the certified value according to half absolute relative difference (HARD, i.e. $[(\text{analysis}_1 - \text{analysis}_2)/(\text{analysis}_1 + \text{analysis}_2)]$; Stanley and Lawie, 2007) which is <0.05 for all analytes apart from Be and Cu. In terms of precision, the percent relative standard deviation (RSD%) or covariance for analysis of OREAS 24b is <10% for all analytes apart from As, Cu, Ni, Sc and Zn. Similar levels of agreement were found for parent–duplicate pairs. All blank values were less than three times the lower level of detection.

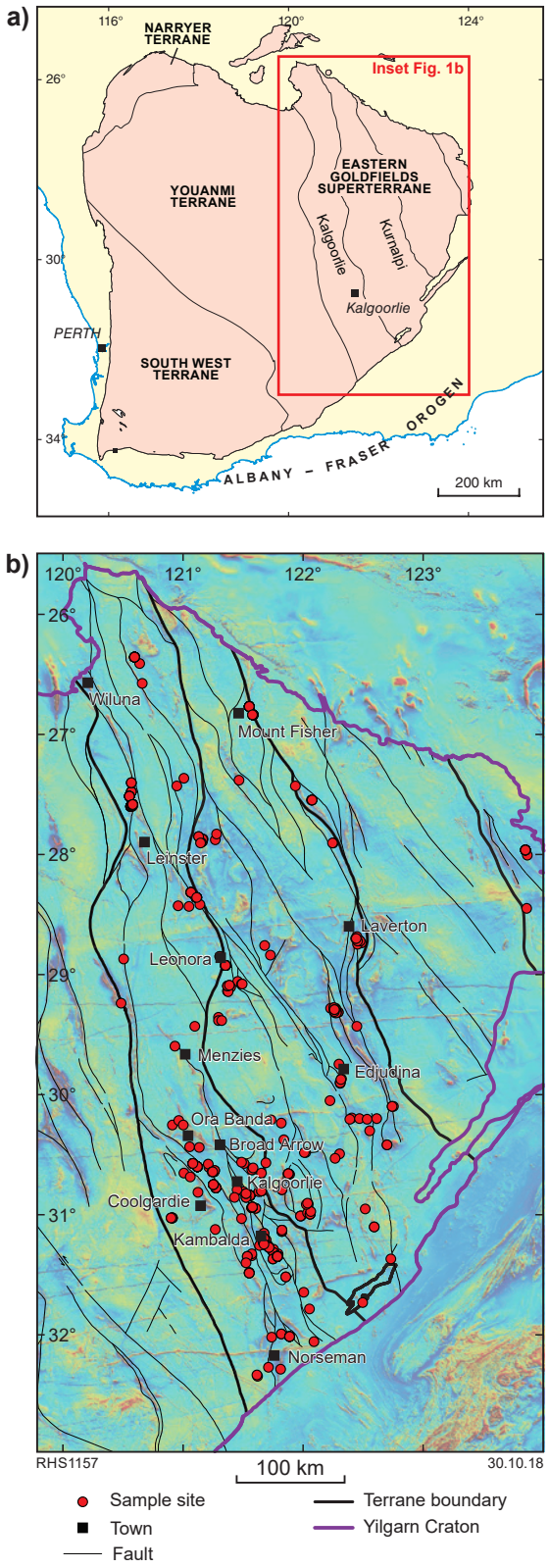

Figure 1. Location of samples within the Eastern Goldfields Superterrane (EGST): a) terrane subdivision of the Yilgarn Craton; b) aeromagnetic image of the EGST showing the locations of samples used for this study. Note that many sites represent the location of a diamond drillhole, cores from which commonly yielded several samples

Alteration

Although samples collected under the Eastern Goldfields greenstone geochemical barcoding project reflect the freshest available material, all have undergone variable amounts of recrystallization at greenschist facies and in some cases up to amphibolite facies metamorphism, and potentially, variable pre- and post-metamorphic hydrothermal alteration. Visibly veined, or clearly hydrothermally altered material was avoided during sampling, but the cryptic effects of hydrothermal alteration are unavoidable, particularly because of the dependence sampling has had on drillcore from mineral exploration targets. These effects potentially include significant changes to the primary concentrations of fluid-mobile elements.

Analysed LOI includes rare (eight samples) values >10 wt%, but >75% of samples have LOI <3 wt% (>60% with LOI <2 wt%), suggesting alteration effects on the majority of analysed rocks are not significant. Furthermore, there is no clear correlation between LOI and either the LILE, HFSE or REE concentrations. All major element data used here has been recalculated on a volatile-free (anhydrous) basis; thus, for example, MgO (in wt%) is quoted as '*a*MgO'. Samples with both >60 wt% $a SiO_2$ and aK_2O+aNa_2O <4 wt% (or aNa_2O <1 wt% or aK_2O <0.2 wt%) were removed as such values almost certainly indicate significant alkali loss. For similar reasons, samples with an Aluminium Saturation Index [ASI = molecular ratio of $Al_2O_3/(CaO+Na_2O+K_20)$] >1.2 were removed from the dataset. This still permits inclusion of samples that are moderately peraluminous (i.e. ASI >1), as most felsic magma series naturally evolve from metaluminous to weakly peraluminous compositions at >70 wt% SiO_2. All samples with $aSiO_2$ >77 wt% were also removed from the dataset, as these most likely are either silicified rocks or epiclastic/clastic rocks. Although potential alteration trends in specific rock groups or at specific location might easily be obscured within the large regional dataset, the broad geochemical patterns observed appear most consistent with igneous processes and suggest that our sampling strategies have significantly minimized the number of samples with whole-rock compositions that have been significantly affected by hydrothermal alteration.

Sample coverage, age and description

Our present interest in the geochemistry of lamprophyric rocks within the EGST stems from the observation that although their distribution throughout the EGST is very uneven, it is regional, and hence the incompatible trace-element signatures of these rocks might yield information on widespread compositional variations within lithospheric mantle domains. In view of this, lamprophyric rocks are now being routinely sampled as part of the Eastern Goldfields greenstone geochemical barcoding project, and spatial (and potential temporal) variations in these remains a focus for further work. Rocks that can be broadly texturally classified as lamprophyric (i.e. distinctly hornblende–, biotite– or hornblende–biotite–porphyritic, fine-grained mafic rocks) are particularly common in diamond drillcore as dykes that cut the greenstone sequence of the Hannans Subgroup (Kalgoorlie Group), from the Kambalda region (Fig. 2a,b). Here, lamprophyre intrusions into the greenstone sequence have been dated between c. 2.68 and 2.64 Ga (Perring et al., 1989; Perring and McNaughton, 1992; Taylor et al., 1994). At Kalgoorlie, hornblende lamprophyre dykes intruded greenstone sequences at least between c. 2.65 and 2.64 Ga (Vielreicher et al., 2016). In drillcore from the Kambalda and Kalgoorlie region, and elsewhere in the EGST, aphyric to weakly amphibole-phyric mafic rock, not clearly texturally identifiable as lamprophyre (Fig. 2c,d), also forms sills and flows within volcanic units, including in the lower parts of the BFG, and is compositionally identical to the hornblende lamprophyres. Given current constraints on the age of the BFG (c. 2.692 – 2.66 Ga, with the oldest direct magmatic age being 2.681 Ga [Nelson, 1997b]), which overlies the Hannans Subgroup, this potentially extends lamprophyre-type magmatism closer to c. 2.68 Ga.

Taylor et al. (1994) noted that Archean lamprophyres in the EGST included hornblende-macrocrystic varieties that are predominant in the southern Kalgoorlie Terrane, and biotite-macrocrystic varieties that dominated the central to northern Kurnalpi Terrane. Figure 3a shows the distribution of 15 hornblende–, biotite– or hornblende–biotite–porphyritic, fine-grained, mafic rocks that have been broadly classified from hand sample as lamprophyric, collected so far as part of the Eastern Goldfields greenstone geochemical barcoding project. Also shown is the distribution of sills and flows of aphyric to weakly amphibole-phyric mafic rocks that are compositionally identical to the lamprophyric rocks, and that either lie within the BFG (seven samples denoted 'enriched mafic BFG', Fig. 3a — 'enriched' is used in reference to high concentrations of aP_2O_5, LILE and LREE) or outside of exposures interpreted as part of the BFG (eight samples denoted 'enriched mafic volcanic').

In the Kambalda region, intrusions of broadly dioritic and monzodioritic composition are commonly associated in drillcore with lamprophyric rocks (e.g. Perring et al., 1989; Perring and Rock, 1991). These typically range from hornblende ± plagioclase to plagioclase–hornblende–porphyritic rocks comprising sub- to euhedral hornblende ± plagioclase to 8 mm, and hornblende aggregates and mafic clots to 1 cm, in a fine- to medium-grained groundmass of plagioclase and, in more silica-rich rocks, quartz (Fig. 2e,f). They are texturally and mineralogically transitional with the hornblende lamprophyric rocks, with which they appear comagmatic (e.g. Perring et al., 1989). These rocks are identified in Figure 3a as 'enriched diorites' (29 samples).

Felsic volcanic rocks form a major stratigraphic component of the BFG throughout the Kalgoorlie Terrane and contemporaneous, subvolcanic, feldspar (± hornblende) porphyritic rocks of broadly granodioritic composition are also locally abundant. The distribution, description, geochronology and stratigraphic relationships of these rocks has recently been thoroughly documented (Tripp, 2013). Felsic rock samples from the BFG are subdivided in Figure 3b,c based on geochemical criteria into 'enriched felsic BFG' (98 samples), 'potentially enriched felsic BFG' (seven samples) and 'unenriched felsic BFG' (33 samples). Compositionally similar volcanic rocks within the EGST lying outside of exposures interpreted to form part of the BFG are denoted 'enriched felsic volcanic' (21 samples),

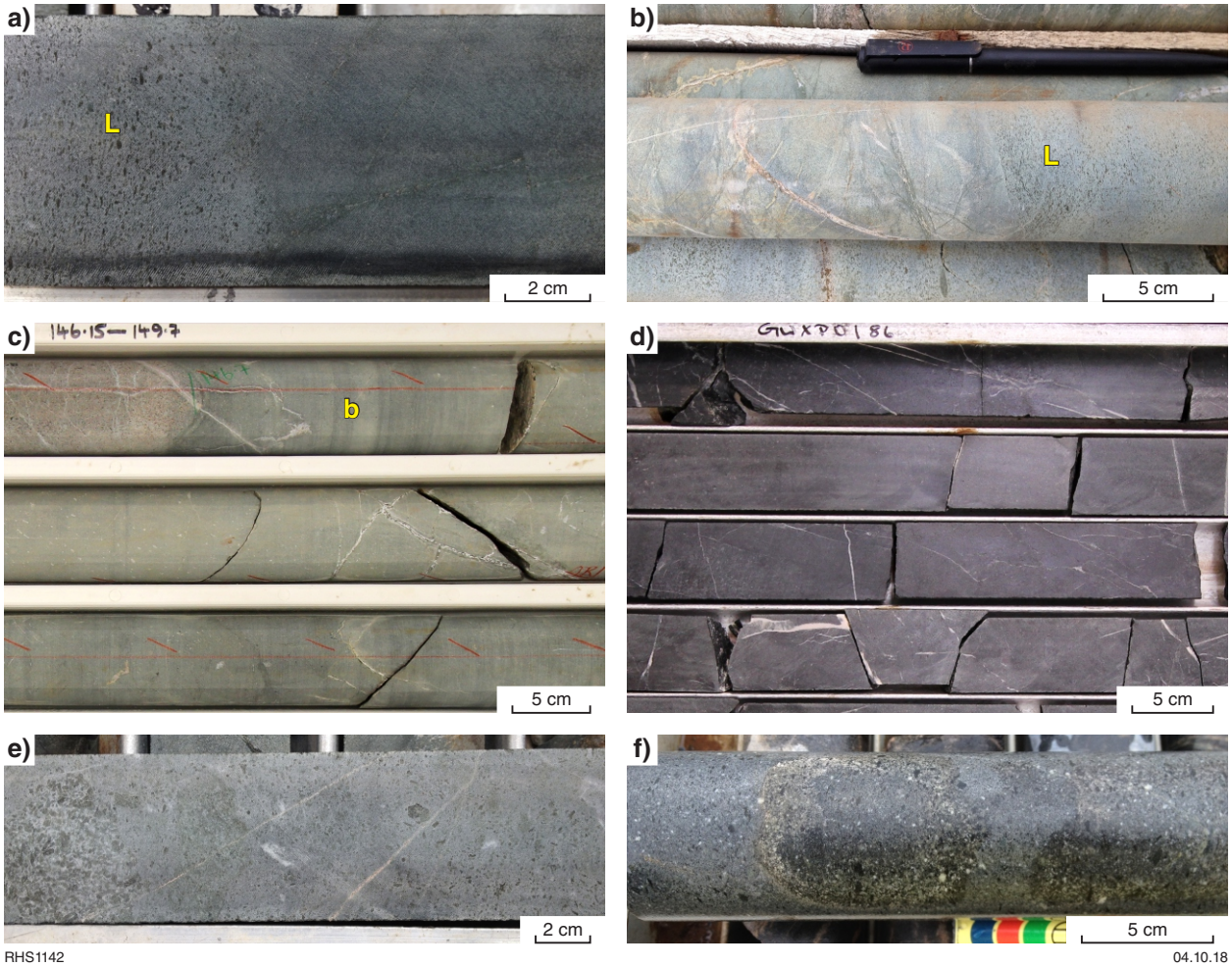

Figure 2. **Photos of diamond drillcore: a) and b) show contacts between lamprophyric dykes (L) and basalt (from CD65056A and LD7006 respectively); c) contact between a crystal-rich felsic volcanic rock of the BFG and a very fine-grained mafic intrusion (b), compositionally identical to the lamprophyric rocks (from 12GMSD001); d) a massive, aphyric, basalt unit, compositionally identical to the lamprophyric rocks (from GWXP0186); e) hornblende-porphyritic dioritic or monzodioritic intrusion into basalt (from CD65056A; note cumulate-textured, hornblende-rich, cognate xenolith); f) hornblende-plagioclase porphyritic dioritic intrusion into basalt (from CD65056A; note abundant rounded cognate xenoliths)**

'potentially enriched felsic volcanic' (13 samples) and 'unenriched felsic volcanic' (261 samples) rocks. These are distributed throughout the EGST and include samples from various volcanic complexes including the Melita Formation (2684 – 2681 Ma; Brown et al., 2002; Baggott, 2006), Teutonic Bore Formation (2692 Ma; Nelson, 1995a), Spring Well Formation (2694 – 2690 Ma; Nelson, 1997a; Kositcin et al., 2008) and the Little Peters Formation (< 2682 Ma).

Similarly, feldspar (± hornblende) porphyritic subvolcanic intrusions within the felsic volcanic piles are subdivided geochemically into 'enriched felsic intrusions' (105 samples), 'potentially enriched felsic intrusions' (25 samples) and 'unenriched felsic intrusions' (68 samples).

Geochemical characteristics

At relatively low-silica values (aSiO$_2$ <56 wt%) the lamprophyric rocks and compositionally equivalent aphyric to weakly amphibole-phyric mafic rocks (enriched mafic BFG and enriched mafic volcanic rocks) show a wide range of aMgO concentrations (3.9 to 14.7 wt%) and Mg$^{\#}$ (45 to 76) and high concentrations of Ni (up to 418 ppm) and Cr (up to 1060 ppm) (Fig. 4). Most have primitive compositions with aMgO (> ~7 wt%) and high Mg$^{\#}$ (>60) reflecting equilibration with mantle peridotite. Only 7% of samples have K_2O/Na_2O >1 and approximately half have ratios <0.5 (Fig. 4). Although aK_2O varies considerably (0.19 to 3.45 wt%), 41% of samples are medium-K and 17% are low-K rocks. Within this compositional range for EGST lamprophyric rocks, most samples from the Mount Fisher greenstone belt, along the northeastern edge of the Kurnalpi Terrane, cluster in a distinct field characterized by low Mg$^{\#}$ (mostly <50) and low aMgO (mostly <6 wt%), Ni and Cr concentrations (Fig. 4). They also account for virtually the entire population of rocks falling within the high-K field.

The relatively low-silica lamprophyric rocks, enriched mafic BFG and enriched mafic volcanic rocks are characterized by strong enrichments in LILE, Th, U and light- to middle-REE (L-MREE) and depletions in heavy

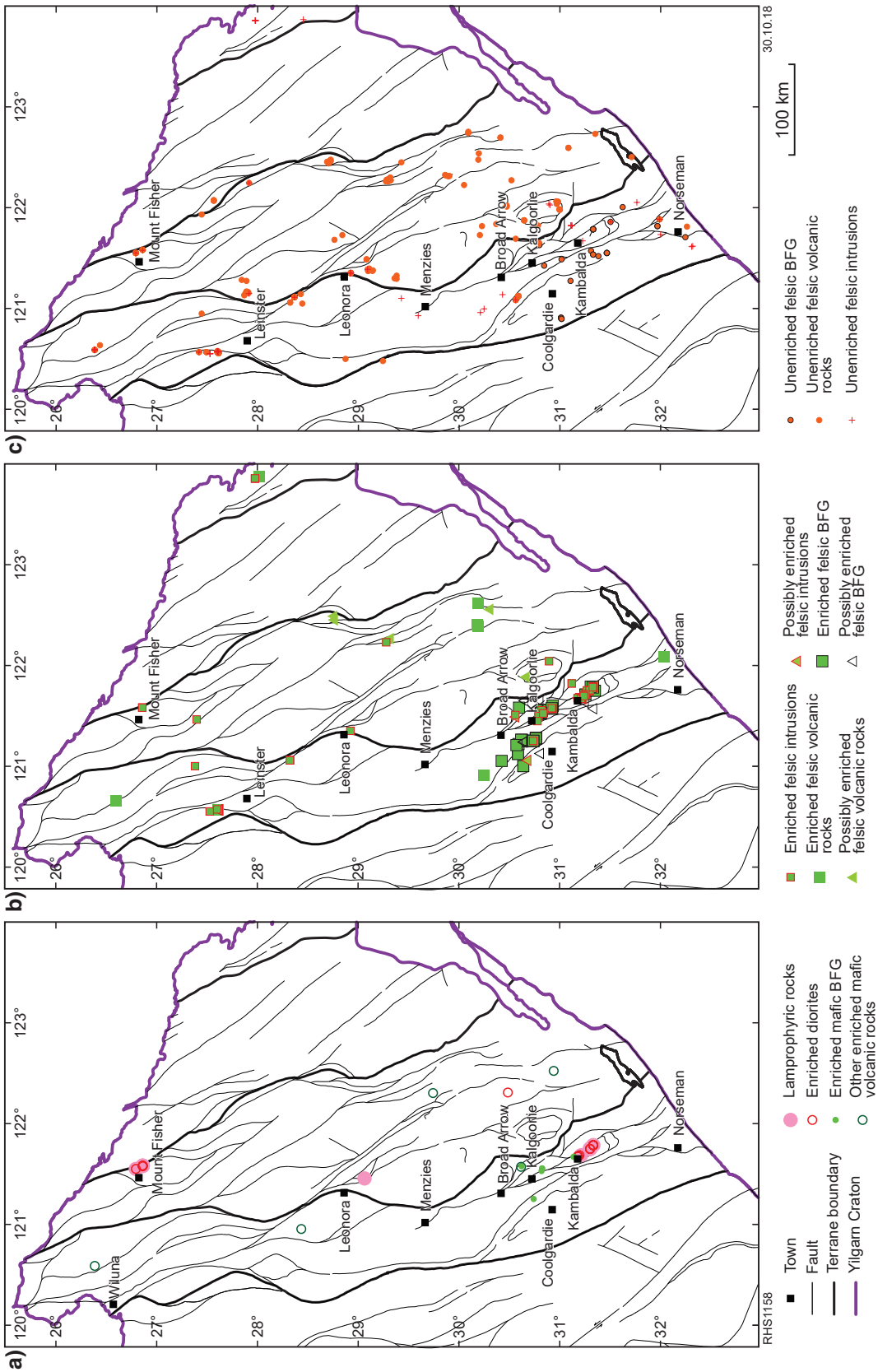

Figure 3. Outline of the EGST showing the locations of: a) lamprophyric rocks and associated mafic to intermediate extrusive and subvolcanic rock; b) samples representing the main compositional group of BFG dacitic rocks, regional equivalents of these, subvolcanic equivalents and possible rhyolitic equivalents; c) felsic volcanic rocks and subvolcanic equivalents compositionally dissimilar to the main compositional group of BFG dacitic rocks. Note that many sites represent the location of a diamond drillhole, cores from which commonly produced several samples. Hence, a single point (or symbol) may represent several samples

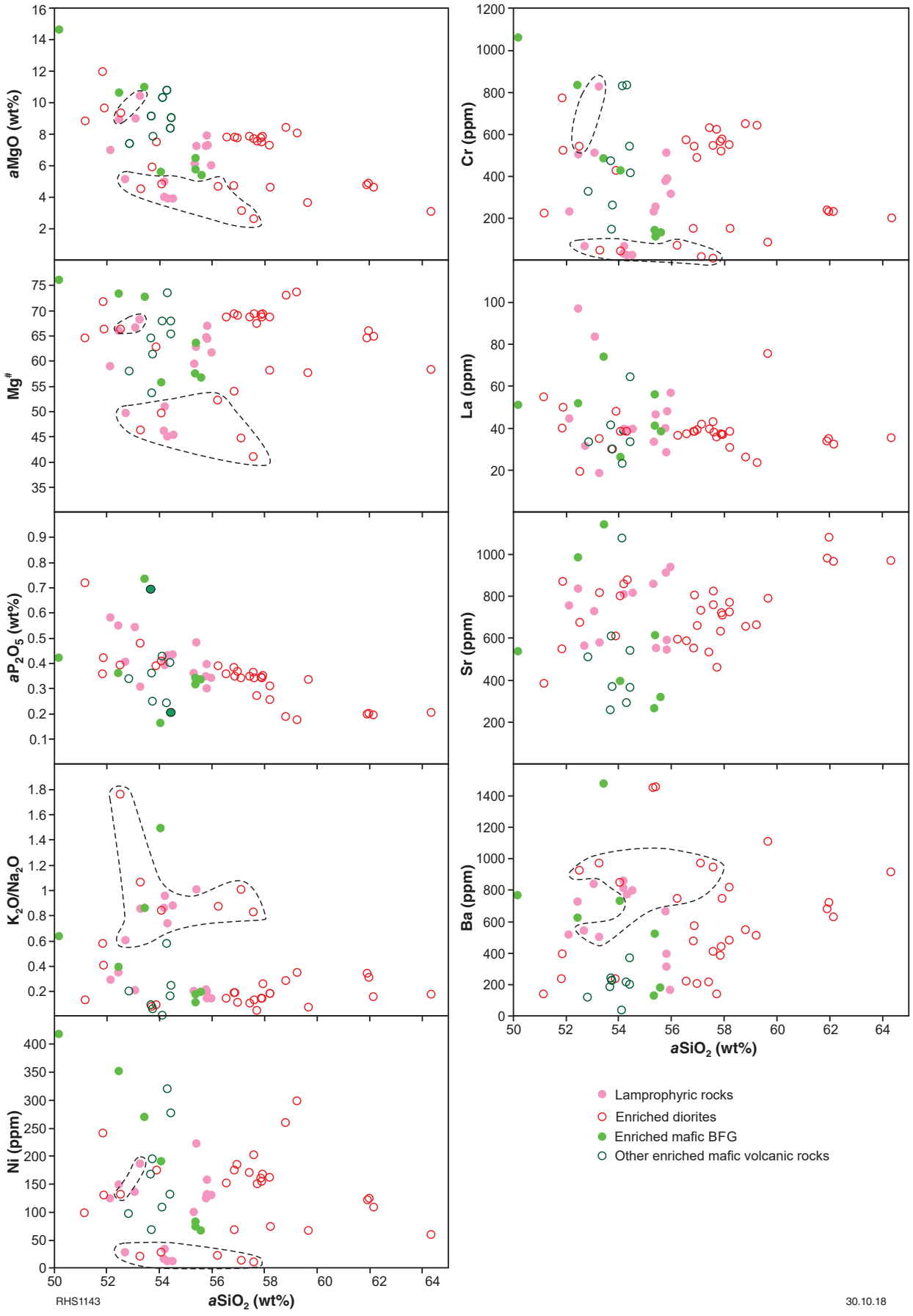

Figure 4. **Variation of selected major elements, major element ratios and trace elements with silica (all major elements reported on an anhydrous basis) for lamprophyric rocks, enriched diorites, enriched mafic BFG rocks and regional equivalents ('Other enriched mafic volcanic rocks'). Fields in some diagrams enclose samples from Mount Fisher. Here, and in subsequent figures, the prefix *a* (e.g. *a*MgO) denotes element oxides that have been recalculated on an anhydrous basis**

REE (HREE; Fig. 5) producing high La/Yb and Dy/Yb ratios. On mantle-normalized incompatible trace-element diagrams, they show distinct negative anomalies for the HFSE (Fig. 5) and for aP$_2$O$_5$. Although most of the HFSEs (excluding Ti) and aP$_2$O$_5$ range to concentrations much higher than in typical mantle-derived (e.g. mid-ocean ridge basalt [MORB]) magmas (Fig. 5), at similar aMgO values and Mg$^{\#}$, HFSE/HFSE ratios (e.g. Nb/Zr) remain very close to those of normal mid-ocean ridge basalt (N-MORB; Fig. 6). This suggests a mantle source that was as melt-depleted as N-MORB sources. None of the samples show distinct Eu anomalies, and Sr anomalies are either absent or range from weakly positive to moderately negative. The rocks from Mount Fisher plot at the high end of the compositional range for K and Ba, consistently have weakly positive Eu anomalies but are otherwise indistinguishable from the other lamprophyric rocks, enriched mafic BFG and enriched mafic volcanic rocks.

Among these rocks, there is no consistent means of distinguishing geochemically between samples showing petrological/textural characteristics of lamprophyres and those aphyric rocks showing no such characteristics, or between intrusions and samples interpreted to be volcanic. Hence the term 'lamprophyre' cannot strictly be used here as a compositional qualifier, and so this compositional group will be referred to here as the 'lamprophyric series'. Perhaps the most reliable means of identifying members of this series from other aphyric basaltic to andesitic rocks of the greenstone sequences, and particularly from 'enriched' high-Th silicic basalts (Barnes et al., 2012) such as the Paringa Basalt that forms a significant stratigraphic interval in the Kambalda–Kalgoorlie region, is the combination of strong enrichments in aP$_2$O$_5$, Sr, Th, Zr and LREE at a given Mg$^{\#}$ or aMgO content (Fig. 7).

The enriched diorites commonly associated with rocks of the lamprophyric series in the Kambalda region (e.g. Perring et al., 1989; Perring and Rock, 1991) also show compositional similarities with the lamprophyric series. This is particularly the case when samples from Mount Fisher are considered separately. In all compositional variation diagrams (but not including the Mount Fisher samples), the fields for enriched diorites either extensively overlap with, or extend, broad compositional trends defined by, the fields for the lamprophyric series (Fig. 4). Both groups have remarkably similar mantle-normalized incompatible trace-element patterns (Fig. 5). The strong compositional similarities between the EGST lamprophyre series and the enriched diorites led Perring and Rock (1991) to conclude that they were directly genetically related, mainly through a process of hornblende fractionation. Our data are consistent with this interpretation although the degree to which the data scatter suggests a range of compositionally distinct initial magma batches. This is perhaps exemplified by the consistent differences between the data population from Mount Fisher and the main population. In addition, on plots of aSiO$_2$ vs either Ni or Cr, many spatially associated enriched diorites and lamprophyric series rocks form significantly better constrained fields (Fig. 8).

Importantly, most of the enriched diorites (including the samples from Perring and Rock, 1991) have the clear compositional characteristics of Archean sanukitoids. Apart from the Mount Fisher rocks, nearly all enriched diorites at ~60 wt% aSiO$_2$ have Mg$^{\#}$ >60 (up to 73), Ni and Cr >100 ppm (up to 298 and 650 ppm respectively) and high concentrations of Sr and Ba (up to 1080 and 1110 ppm respectively; Fig. 4). Previous petrogenetic models interpret sanukitoids as direct low-degree partial melts of lithospheric peridotite, based primarily on the apparent

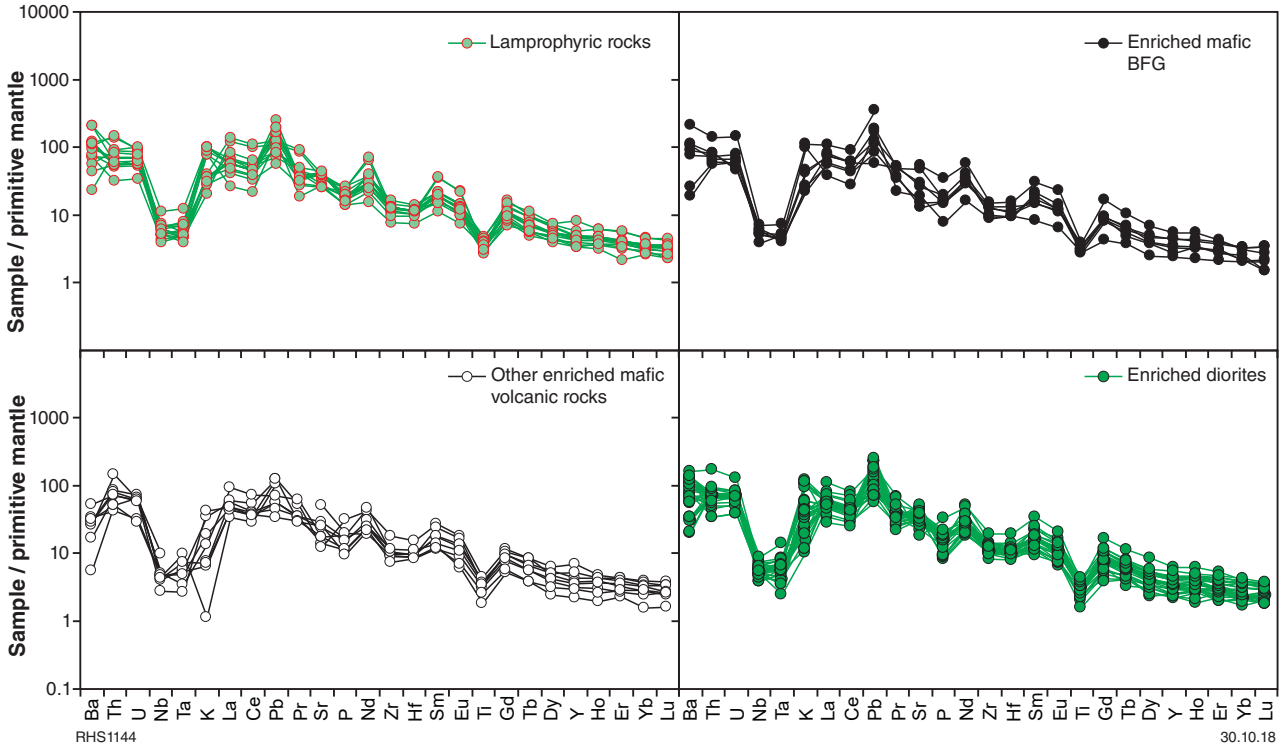

Figure 5. Mantle-normalized multi-element diagrams for lamprophyric rocks, enriched diorites, enriched mafic BFG rocks and regional equivalents (normalizations after Sun and McDonough, 1989)

absence of compositionally suitable mafic parental magmas (e.g. Shirey and Hanson, 1984; Stern et al., 1989; Smithies and Champion, 2000). Archean sanukitoids in the Canadian Superior Province are also spatially and temporally associated with lamprophyres but are not considered to be genetically related because the lamprophyres commonly have similar or lower MgO contents and $Mg^{\#}$ than spatially associated sanukitoids (Stern et al., 1989). This relationship typically does not hold for *spatially associated* lamprophyric rocks and enriched diorites (sanukitoids) in the EGST (Fig. 9) but might become difficult to interpret on a regional basis given the wide compositional ranges observed. As outlined above, data presented here are more consistent with a direct genetic relationship — enriched diorite derived from lamprophyric magmas through hornblende-dominated fractionation (Perring and Rock, 1991) — and challenge the idea that sanukitoids are direct melts of mantle peridotite.

The rocks from Mount Fisher, again, are exceptions, having lower $Mg^{\#}$ and significantly lower Cr and Ni concentrations than typical Archean sanukitoids (Fig. 4). However, they share these characteristics with their associated lamprophyric series, again suggesting a strong source control on magma composition.

Felsic volcanic rocks

Among the most diagnostic compositional characteristics of the combined lamprophyric series and sanukitoid dykes in the EGST is their strong enrichments in aP_2O_5, Sr and LREE (and to a lesser extent Ba), with low Nb concentrations that remain close to N-MORB values (most data between 2 and 5 ppm, c.f. N-MORB concentration of 2.33 ppm; Sun and McDonough, 1989; Fig. 10). On a plot of aP_2O_5 vs Nb (Fig. 11), these rocks fall within a tightly constrained band at higher aP_2O_5/Nb ratios than most Archean igneous rocks.

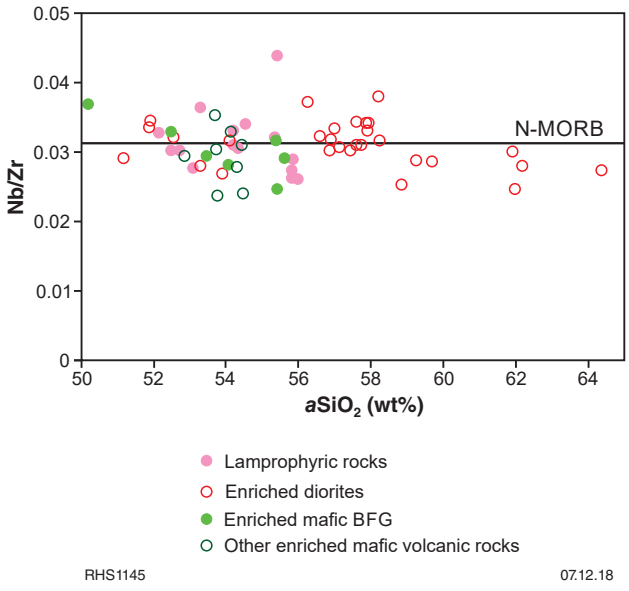

Figue 6. Variation of Nb/Zr with $aSiO_2$ for lamprophyric rocks, enriched diorites, enriched mafic BFG rocks and regional equivalents (solid line represents N-MORB Nb/Zr ratio after Sun and McDonough, 1989)

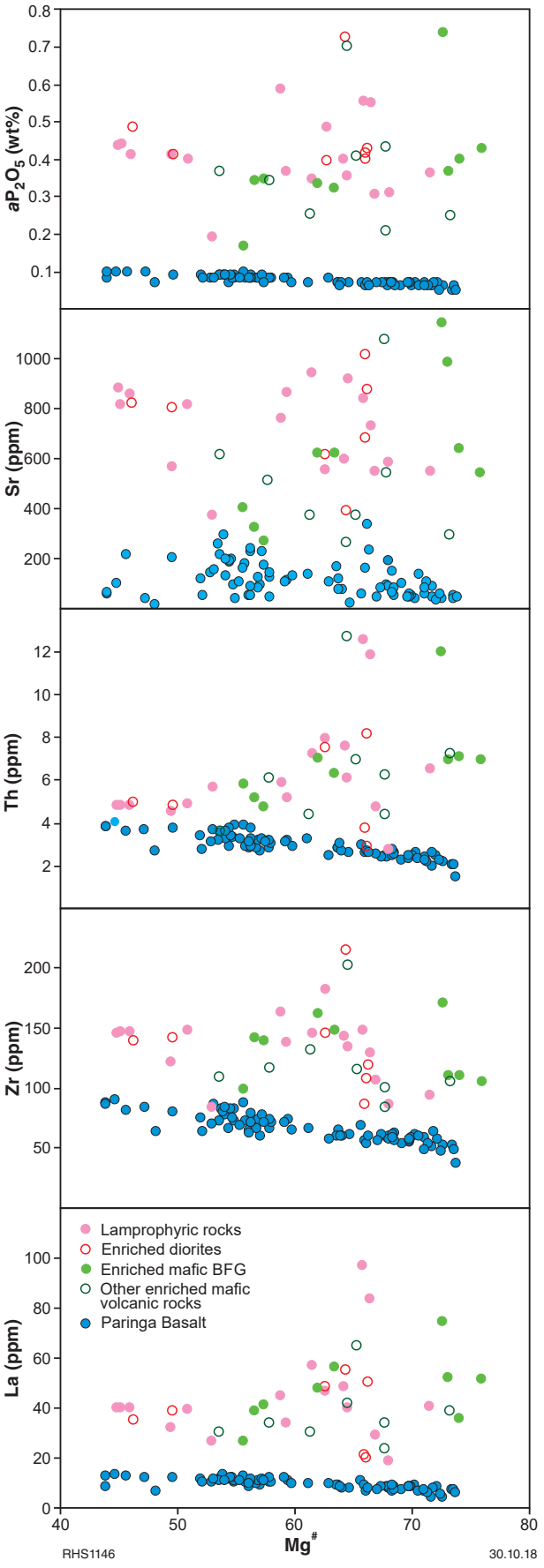

Figure 7. Variation in aP_2O_5, Sr, Th, Zr and La with $Mg^{\#}$ comparing lamprophyric rocks, enriched diorites, enriched mafic BFG rocks and regional equivalents, and with samples of the Paringa Basalt, the most enriched regionally abundant basaltic rock in the EGST

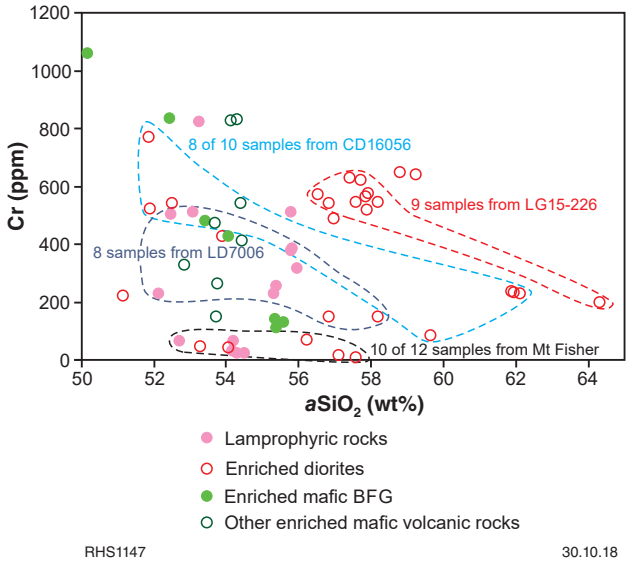

Figure 8. **Variation of Cr with $aSiO_2$ for lamprophyric rocks, enriched diorites, enriched mafic BFG rocks and regional equivalents. Fields outline spatially associated samples. Fields for CD16056, LG15-226 and LD7006 represent samples from drillcores from the Kambalda region, showing that compositionally distinctive magma batches characterize relatively restricted areas**

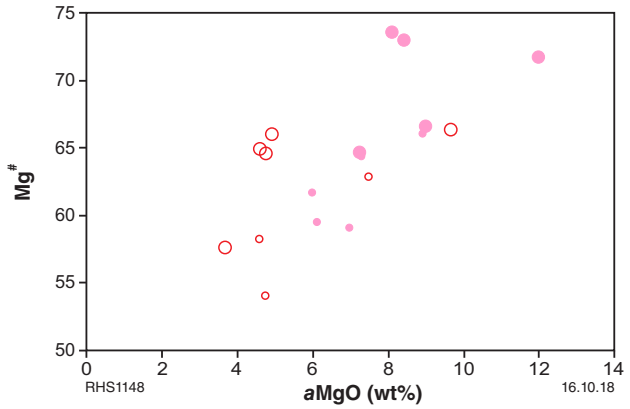

Figure 9. **Variation of $Mg^{\#}$ with *a*MgO for closely spatially associated lamprophyric rocks (open red circles) and associated enriched diorites (sanukitoids – pink circles) from two diamond drillcores taken from the Kambalda region (CD16056A larger symbols; LD7006 smaller symbols). In both cases, when spatially associated magmas are independently assessed, lamprophyric magmas have more primitive compositions than the associated sanukitoids and clearly permit a direct genetic relationship**

Surprisingly, approximately 75% of the samples of BFG volcanic and volcaniclastic rocks lie within the same distinct band. Felsic volcanic rocks, and subvolcanic porphyritic intrusive rocks, with similarly high aP_2O_5/Nb ratios (i.e. enriched felsic volcanic and enriched felsic intrusions) have been sampled at other localities throughout the EGST in both the Kalgoorlie and Kurnalpi Terranes. They are present, for example, northeast of Sir Samuel (Ora Banda Domain), 45 km east of Wiluna (Jundee Domain), northeast of Kurnalpi (Murrin Domain), near Mount Fisher (along the boundary of the Laverton and Duketon Domains) near Tower Hill (Leonora Domain) and ~20 km south-southeast of Bulong (Bulong Domain; Fig. 3). Samples are also present, for example in the Bulong Domain of the Kalgoorlie Terrane, that appear to have ages older than those of the BFG, potentially indicating a protracted or multistage history of high aP_2O_5/Nb magmatism. A dacite sampled approximately 1.7 km northeast of Kanowna Belle, for example, was intercalated with komatiite and yielded a crystallization age of 2708 ± 7 Ma (GSWA 104958, Nelson, 1996). These felsic rocks show compositional features that clearly distinguish them from other felsic volcanic and subvolcanic rocks within the EGST.

Thus, the felsic volcanic rocks of the EGST can be broadly subdivided between at least two major compositional groups (Figs 10, 11); a high aP_2O_5/Nb 'enriched' group (including most samples of the BFG) and a variably lower aP_2O_5/Nb 'unenriched' group sampled from throughout the EGST. The latter include a small (~25%) component of the BFG but also regionally form >60% of EGST felsic volcanic samples (Fig. 3) and include samples with ages between 2.81 and 2.65 Ga (e.g. Czarnota et al., 2010; Fletcher et al., 2001). The relative abundance of low aP_2O_5/Nb rocks is almost certainly an underestimate given our present sample bias towards the Kalgoorlie–Kambalda region where high aP_2O_5/Nb volcanic rocks seem particularly common.

Mantle-normalized trace-element plots are particularly useful in showing the contrasting geochemical characteristics of the two broad groups (Fig. 12). The enriched, high aP_2O_5/Nb, group as well as the EGST lamprophyric series and sanukitoid dykes have very similar normalized trends characterized by strong enrichments in LREE, high La/Yb and Dy/Yb ratios, significant negative Nb anomalies, weak to moderate negative Zr and P anomalies, negligible Eu anomalies and weak negative to positive Sr anomalies (Figs 5, 12). In comparison, the unenriched, low aP_2O_5/Nb, group shows a range of different patterns, suggesting that this is a composite group comprising several discrete magmatic lineages. However, most of the unenriched rocks are characterized by typically lower La/Yb ratios, significantly lower Dy/Yb ratios, larger negative P, Eu and Sr anomalies, and no clear Zr anomaly. The two groups can also be distinguished based on their range of La/Nb ratios (Fig. 13a). The enriched, high aP_2O_5/Nb, group as well as the EGST lamprophyric series and sanukitoid dykes almost invariably have La/Nb ratios above six and show a wide scatter. By comparison, most rocks of the unenriched, low aP_2O_5/Nb, group have La/Nb ratios below 5, forming a relatively tightly constrained array on

a plot of La/Nb vs $a\mathrm{SiO_2}$, with a distinct gap between the two populations over a large silica range (up to ~67 wt% $a\mathrm{SiO_2}$). Furthermore, the enriched and unenriched felsic volcanic groups show strongly contrasting trends on a plot of La/Nb vs Nb (Fig. 13b); the former showing highly variable La/Nb at relatively constant and low Nb concentration (mostly <5 ppm), and the unenriched group showing highly variable Nb concentrations (up to 20 ppm) at La/Nb ratios mostly below 5.

Some styles of alteration, notable those associated with iron oxide–copper–gold (IOCG)-style mineralization, appear to lead to net gains in $\mathrm{P_2O_5}$, along with Fe and K, forming apatite–magnetite–biotite alteration assemblages (e.g. Corriveau et al., 2016). Such assemblages are also noted in association with gold mineralization throughout the EGST (Fig. 14a). Hence, it is important to establish that the distinct compositional features of the enriched rocks are not a result of alteration, particularly since a high proportion of samples are from drillcores that tested mineral exploration targets. Notably, the mafic (lamprophyric) to felsic enriched rocks form a very tight array on a plot of Nb vs $a\mathrm{P_2O_5}$ (Fig. 11). This group contains many samples that are clearly texturally and compositionally little altered (e.g. Fig. 2e,f). Even in pervasively sericitized volcanic and volcaniclastic examples of the BFG, apatite can remain as large, euhedral, crystals (Fig. 14b), attesting to the stability of apatite under the conditions of alteration relevant to most samples considered here. The well-constrained $a\mathrm{P_2O_5}$/Nb array is consistent with the very well-constrained mantle-normalized trace-element plots for these rocks (Figs 5, 12), particularly compared with the unenriched rocks. This, for the enriched rocks, points to only minor alteration. In addition, whereas apatite–magnetite–biotite alteration assemblages are associated with gold mineralization in the EGST, the high-$a\mathrm{P_2O_5}$ enriched rocks are generally lower in Fe than the unenriched rocks, although $a\mathrm{P_2O_5}$ correlates positively with Fe since both are typically enriched in the more mafic end of the magmatic spectrum (Fig. 15). There is also no indication that $a\mathrm{P_2O_5}$ correlates with typically fluid-mobile elements such as Ba, S, As etc. (Fig. 15), but remains relatively tightly correlated with fluid-immobile elements such as Nb (Fig. 11), Y and $\mathrm{TiO_2}$ (Fig. 15).

Of the few low $a\mathrm{P_2O_5}$/Nb 'unenriched' samples with La/Nb above 6 (Fig. 13), most either come from Mount Fisher or from two diamond drillcores from the Agnew region and have potentially been misclassified here. Since $a\mathrm{P_2O_5}$ content forms an important factor discriminating between the two main groups of volcanic rocks, and decreases rapidly with increasing $a\mathrm{SiO_2}$, identification of samples belonging to the high $a\mathrm{P_2O_5}$/Nb group becomes difficult in rocks with >70 wt% $a\mathrm{SiO_2}$. For this reason, high-silica samples with $a\mathrm{P_2O_5}$/Nb >0.062 **and** La/Nb >6 are denoted here as 'potentially enriched' felsic rocks (e.g. Fig. 3). It is possible that some of the high-silica unenriched rocks, including many of the anomalous samples from Mount Fisher and Agnew, should also be classified as 'potentially enriched'.

Most significantly, when compared to the EGST lamprophyric series and cogenetic sanukitoid dykes, the high $a\mathrm{P_2O_5}$/Nb 'enriched' group of felsic volcanic rocks (and associated porphyritic subvolcanic intrusions), including the dominant BFG population, also shows the distinct geochemical characteristics defining sanukitoids (Fig. 10). Although there is some overlap between the broad compositional fields defined by the enriched and unenriched rock populations, the unenriched felsic rocks are typically much less like sanukitoid. Thus, at ~60 wt% $a\mathrm{SiO_2}$, most of the enriched rocks have higher $\mathrm{Mg^{\#}}$ (55–69) and higher concentrations of Cr (140–500 ppm), Ni (50–250 ppm), Ba (300–1400 ppm) and Sr (400–1100 ppm) compared with most of the unenriched rocks ($\mathrm{Mg^{\#}}$ = 40–60; Cr = 20–170 ppm; Ni = 20–150 ppm; Ba = 30–1000 ppm; Sr = 400–1100 ppm).

Thus, our data suggest that as much as 75% of the magmatic component of the BFG are high-Mg andesites and high-Mg dacites, and are the volcanic equivalents of sanukitoid. Although data from outside of the Kalgoorlie–Kambalda region are fewer, the preliminary suggestion is that similar high-Mg andesites and high-Mg dacites form a significant proportion of the felsic volcanic rock population.

Composition variations within the Black Flag Group

We have not yet investigated in detail the potential stratigraphic compositional variations within the BFG although this will be a future component of the Eastern Goldfields greenstone geochemical barcoding project. It is, however, interesting to note that unenriched rocks within the BFG dominate in a north-northwest band immediately west of, and parallel with, the Kambalda dome.

In the case of some diamond drillcores in which the BFG has been sampled in detail, distinct geochemical variations with stratigraphic height are noted. For example:

- In drillhole CD16056, from the Kambalda area, only unenriched volcanic rocks were sampled in the depth interval from 89 to 172 m, but enriched volcanic rocks, locally with voluminous enriched felsic intrusions dominate the remaining depth interval to >1450 m
- In SE18, from the Kalgoorlie area, the intersection of the BFG is almost entirely of enriched volcanic rocks; however, in the upper interval, from 75 to 300 m, these rocks have distinctly higher $a\mathrm{P_2O_5}$ concentrations ($a\mathrm{P_2O_5}$ >0.2 wt%) than in the lower interval, to >1500 m ($a\mathrm{P_2O_5}$ <0.2 wt%).

Such stratigraphic variations may provide a basis for future chemostratigraphic correlations.

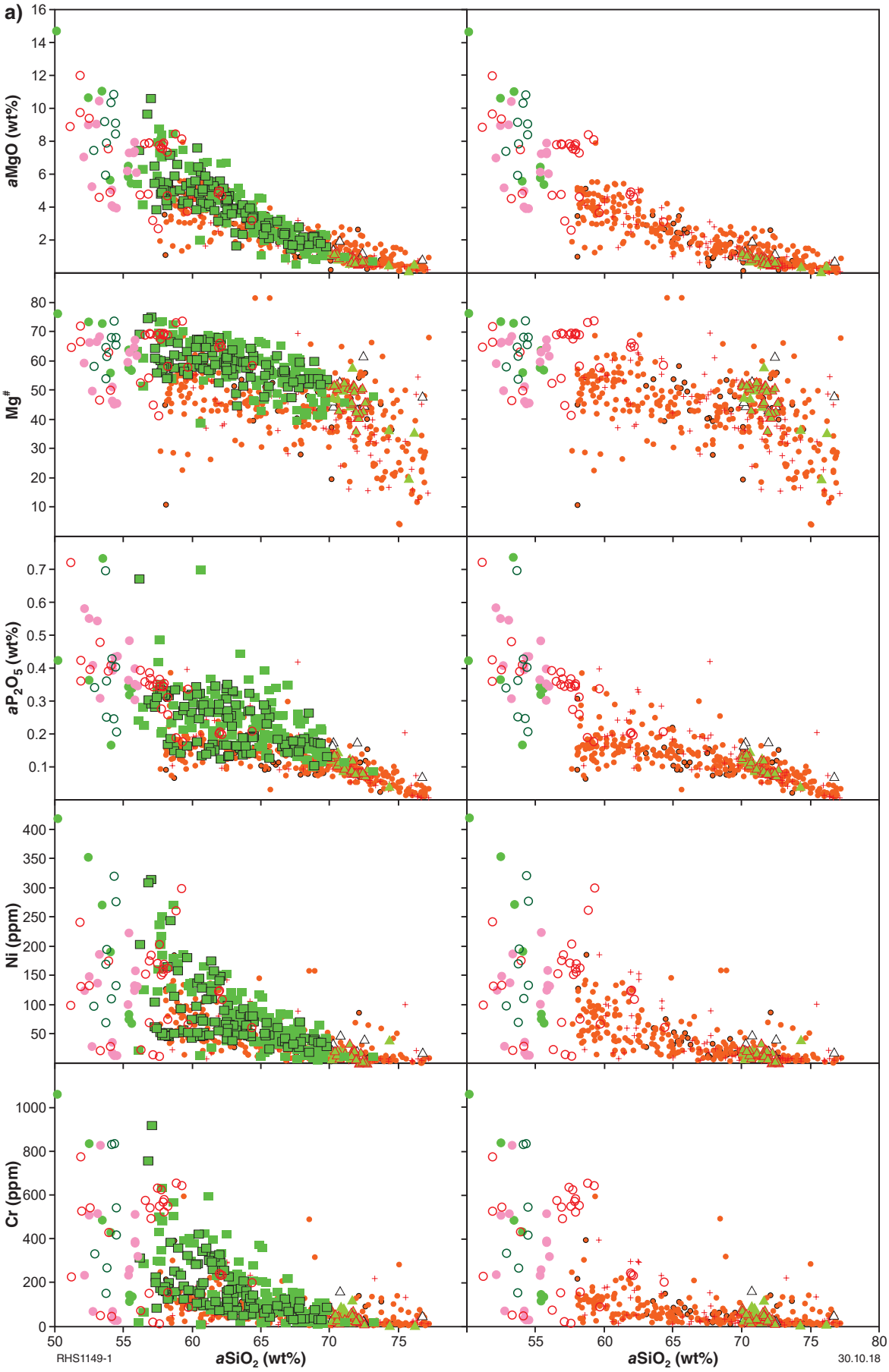
a)
aMgO (wt%)
Mg#
aP2O5 (wt%)
Ni (ppm)
Cr (ppm)
aSiO2 (wt%)
aSiO2 (wt%)
RHS1149-1
30.10.18

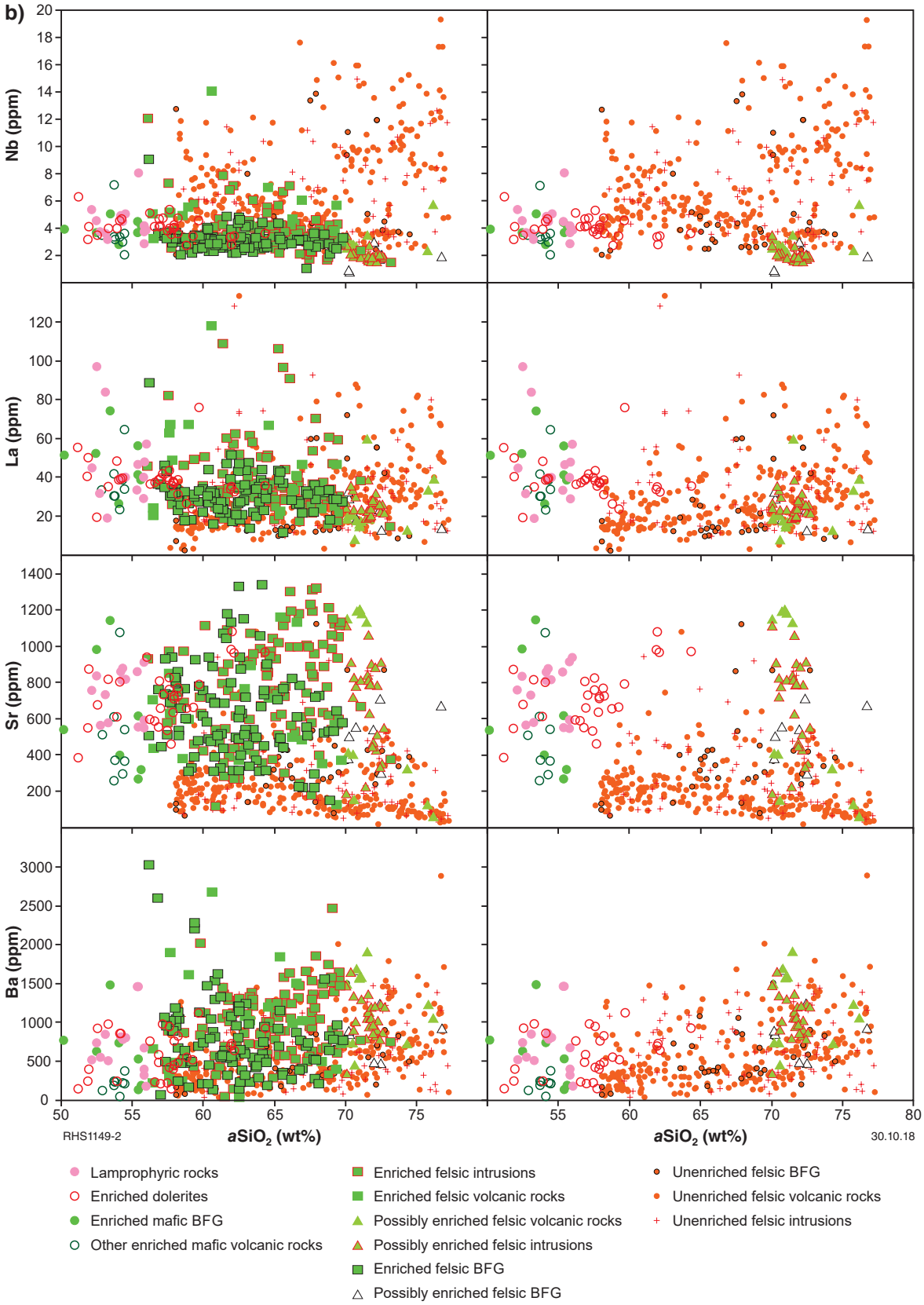

Figure 10. a) page 12; b) above. Variation of selected major elements, major element ratios and trace elements with silica (all major elements reported on an anhydrous basis). Plots on the left show all data. Data for the enriched felsic rocks (volcanic and subvolcanic) have been removed from the plots on the right so that the compositional range of the unenriched felsic rocks can be more readily distinguished

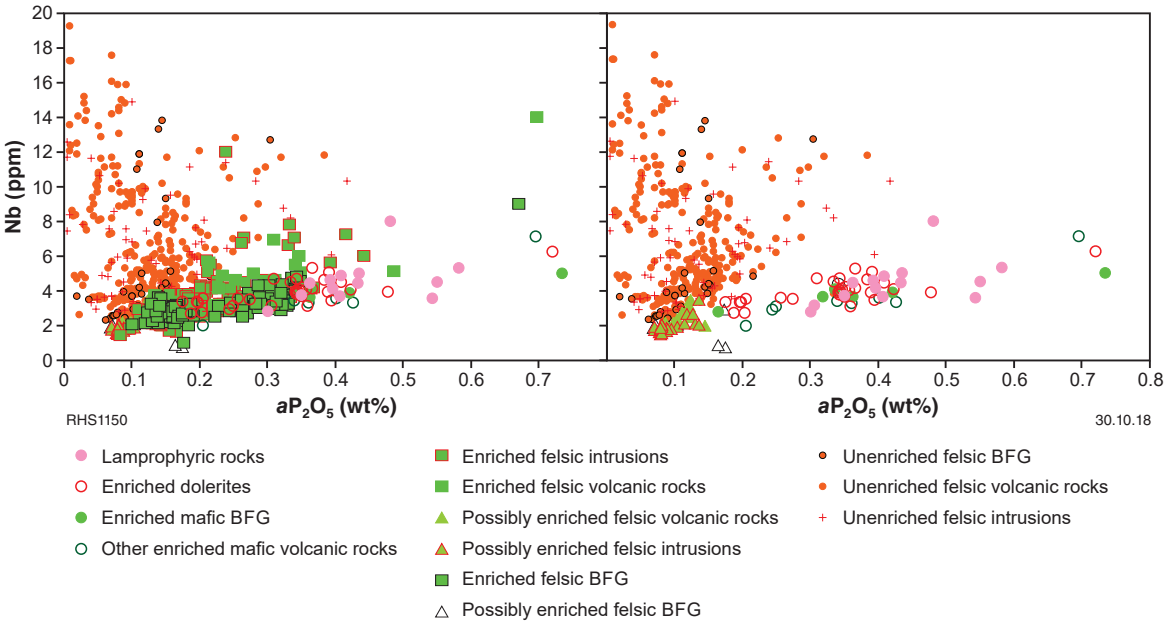

Figure 11. Variation of Nb with aP_2O_5. Plot on the left shows all data. Data for the enriched felsic rocks (volcanic and subvolcanic) have been removed from the plot on the right so that the compositional range of the unenriched felsic rocks can be more readily distinguished

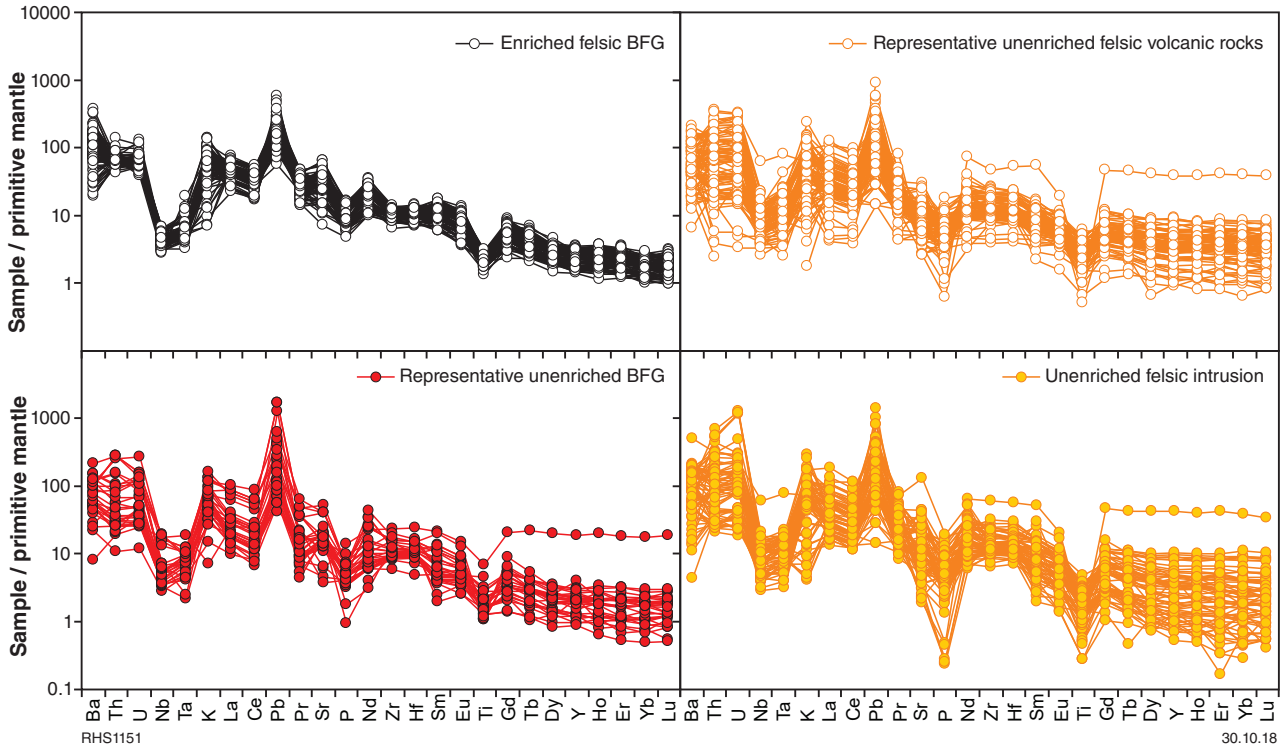

Figure 12. Mantle-normalized multi-element diagrams for enriched and unenriched felsic rocks (normalizations after Sun and McDonough, 1989)

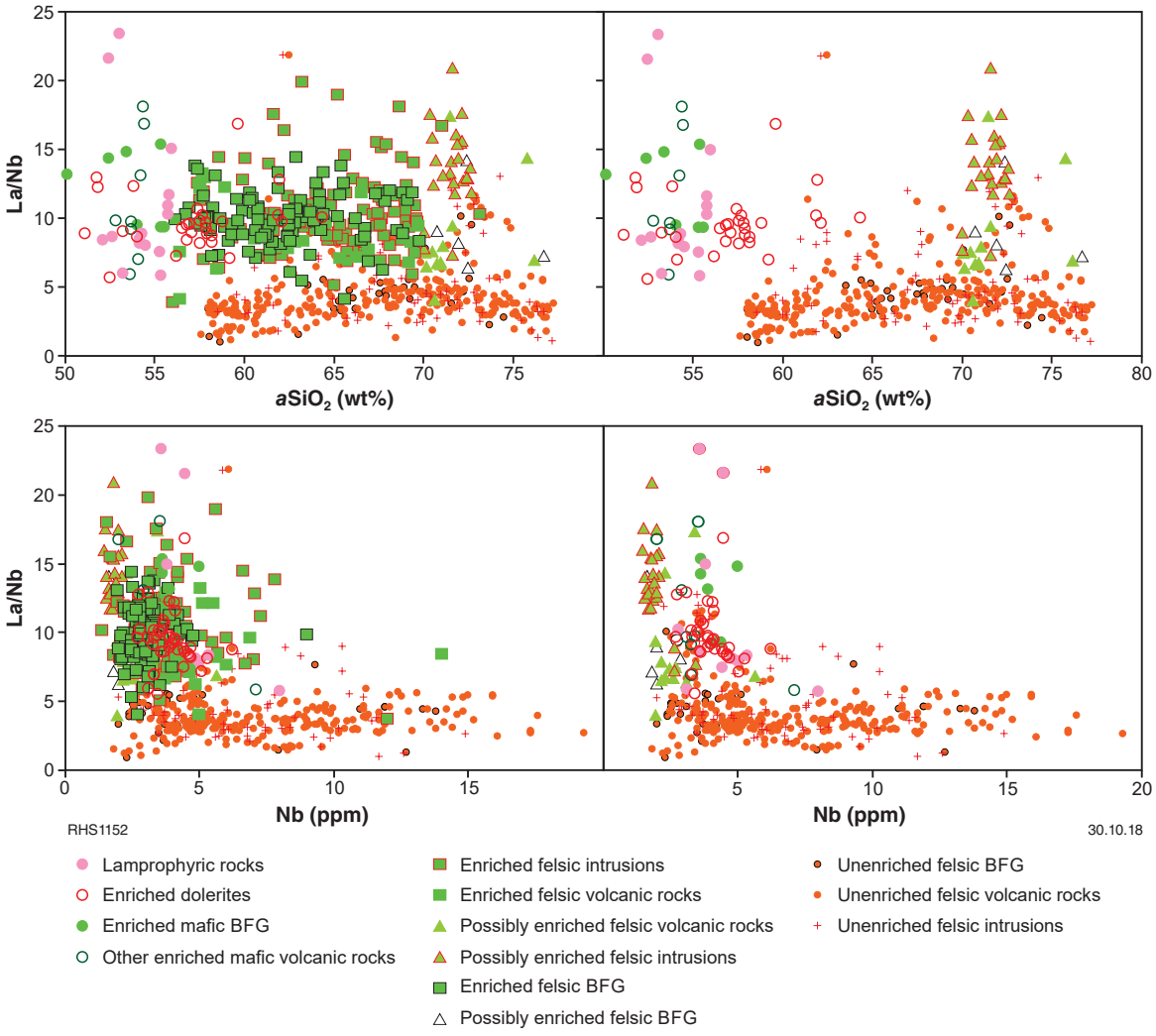

Figure 13. Variation of La/Nb with $aSiO_2$ and with Nb. Plots on the left show all data. Data for the enriched felsic rocks (volcanic and subvolcanic) have been removed from the plots on the right so that the compositional range of the unenriched felsic rocks can be better seen

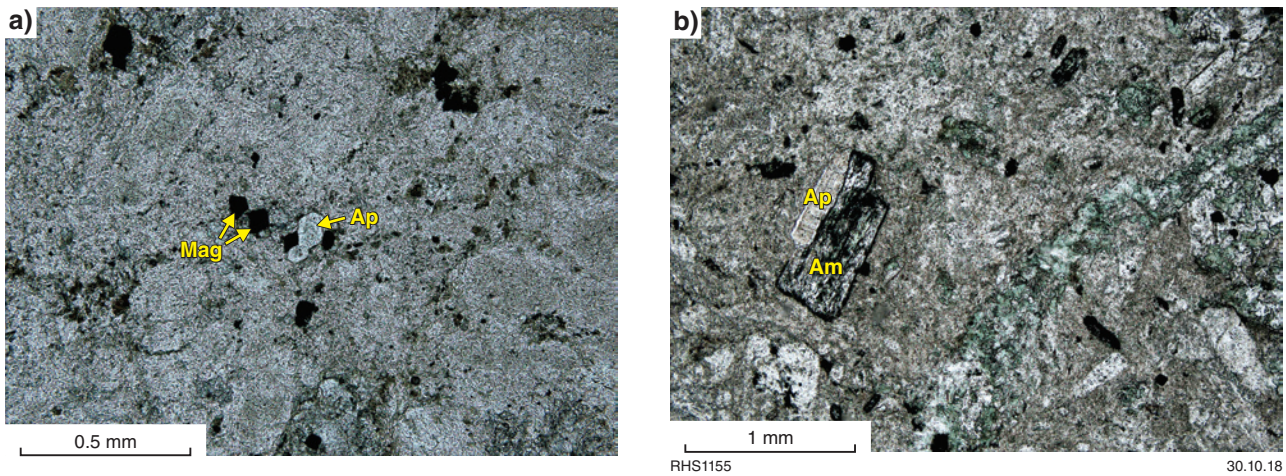

Figure 14. Photomicrographs of volcanic rocks from the BFG showing: a) apatite (Ap)–magnetite (Mag)–biotite assemblages forming stringers and clusters; b) euhedral igneous apatite partially enclosed in altered hornblende (Am) preserved in strongly chlorite–chlorite-altered rock (images courtesy of Alicia Verbeeten, with permission from Northern Star Resources Ltd)

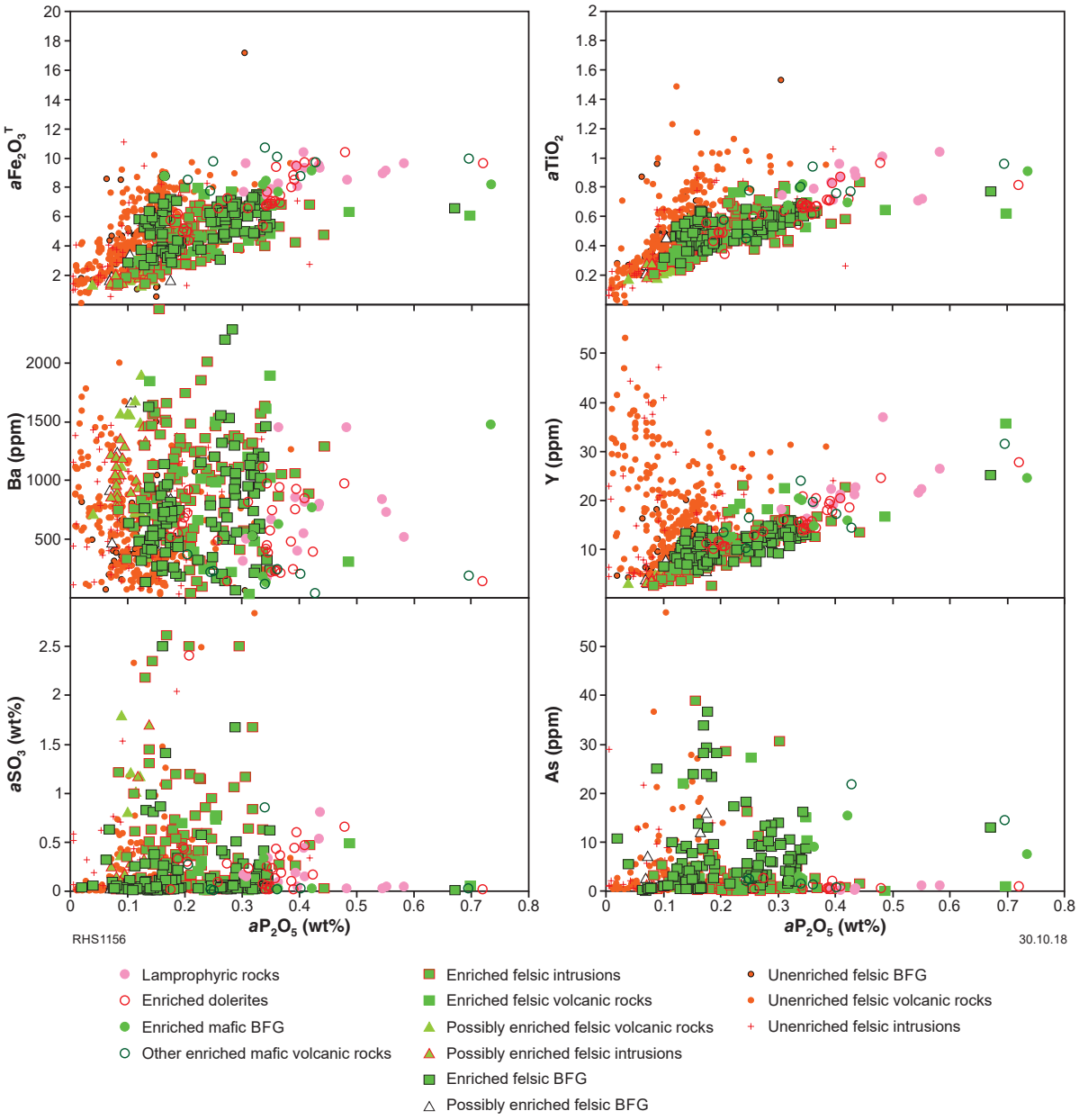

Figure 15. Variation of aP_2O_5 with total Fe (as $aFe_2O_3^T$), Ba, SO_3, As, $aTiO_2$ and Y

Discussion

Our data suggest that the Archean felsic (andesitic to rhyolitic) volcanic rocks of the EGST can be broadly subdivided into an 'enriched' series comprising sanukitoid-like rocks (high-Mg andesite and dacite) and other high-$Mg^{\#}$, -Ni, -Cr, -P and -Sr rocks with high La/Nb >6, and an 'unenriched' series comprising a range of compositions but typically with lower $Mg^{\#}$, Ni, Cr, P and Sr and with La/Nb <5.

Barnes and Van Kranendonk (2014) noted that many Archean andesitic to dacitic rocks of the Yilgarn Craton have on average higher concentrations of Cr and Ni and higher $Mg^{\#}$ than post-Archean subduction-related calc-alkaline volcanic rocks of equivalent silica content. It was suggested that the full compositional range of volcanic rocks in the EGST could be derived through contamination of a mantle plume-derived magma with a composition similar to the voluminous Lunnon Basalt-type low-Th basalt present throughout the EGST, with felsic material similar to rhyolites found in association with komatiites in the Black Swan and Perseverance areas of the Kurnalpi Terrane (Barnes and Van Kranendonk, 2014). In this model, both the felsic contaminant and the modelled evolved magmas fall within the compositional range of the unenriched rocks described here. Despite having higher Ni, Cr, and $Mg^{\#}$ than typical post-Archean volcanic rocks of similar silica content, these nevertheless have lower Ni, Cr, and $Mg^{\#}$ than rocks of the enriched series. To explain the very high Ni and Cr concentrations and high $Mg^{\#}$ of the enriched rocks using this model, the high-Mg magma component would have to have been extremely primitive. More importantly, the enriched rocks typically have aP_2O_5 concentrations much higher than the unenriched rocks (range at 60 wt% $aSiO_2$ = 0.14 – 0.37 wt% cf. 0.07 – 0.25 wt%; Fig. 10) and higher than any other locally or regionally available magmatic rock, except for the EGST lamprophyric series and cogenetic sanukitoids. Furthermore, no form of crustal assimilation can explain trends shown by the enriched magmas towards high-La/Nb ratios at relatively constant Nb concentrations, because it is extremely unlikely that such a Nb-depleted and LREE-enriched source forms more than an extremely minor component of the crust — except in the form of intruding lamprophyric or sanukitoid magmas themselves. Thus, the suggestion that felsic magmas of the EGST result through crustal assimilation into mantle (plume) derived magmas is not relevant to the evolution of the *enriched* magmas, which form a significant proportion of the regional felsic magmatism.

The range of trace-element patterns shown by the unenriched series (Fig. 12) almost certainly suggests this group incorporates magma types from diverse origins. In contrast, the similarity in trace-element patterns between the enriched high-Mg andesites and dacites, their subvolcanic compositional equivalents, the EGST lamprophyric series and the sanukitoids suggests strong petrogenetic links.

Perring and Rock (1991) demonstrated that lamprophyres in the Kambalda region were comagmatic with enriched hornblende diorite and we show that these diorites are indeed sanukitoids. Perring and Rock (1991) also suggested that the lamprophyres and hornblende diorite are related through a liquid line of descent dominated by hornblende fractionation. Our data support this model and invalidate the generalization that Archean calc-alkaline lamprophyres do not have high enough $Mg^{\#}$ to be parental to Archean sanukitoid (Fig. 9; e.g. Stern et al., 1989). Most surprisingly, our data suggest that as much as 75% of the magmatic component of the BFG are high-Mg andesites and high-Mg dacites and are the volcanic equivalents of sanukitoid.

The emplacement age of EGST lamprophyres typically varies from c. 2.68 to 2.64 Ga (e.g. Perring et al., 1989; Perring and McNaughton, 1992; Taylor et al., 1994; Vielreicher et al., 2016). Flow units of aphyric to weakly amphibole-phyric 'basaltic' rock, geochemically equivalent to relatively primitive lamprophyre dykes (enriched mafic BFG) occur in the lower to middle portions of the c. 2.69 to 2.66 Ga BFG. Direct dates from two samples of enriched felsic volcanic rock from the BFG gave maximum depositional ages of 2679 ± 8 Ma (GSWA 179684, Wingate et al., 2010) and 2681 ± 5 Ma (GSWA 112110, Nelson, 1995b). Thus, there is a significant period from at least 2.68 to 2.66 Ga when lamprophyre and sanukitoid intrusion and volcanism occurred. Notably, however, some samples of enriched felsic volcanic rocks from other regions (e.g. a dacite sampled approximately 1.7 northeast of Kanowna Belle; GSWA 104958, Nelson, 1996) might be as old as 2708 ± 7 Ma (Nelson, 1997b). If this is the case, they cannot form part of the BFG, and indicate a significantly older period of enriched magmatism.

Source regions

Calc-alkaline lamprophyres and sanukitoid have both been linked to direct melting of metasomatized lithospheric mantle (e.g. Shirey and Hanson, 1984; Rock and Groves, 1988a,b; Rock et al., 1989; Stern et al., 1989; Smithies and Champion, 2000; Martin et al., 2005). Whereas this model seems appropriate for lamprophyres, it gives sanukitoid the unique status of being the only primary felsic magma thought to be extracted directly from a mantle source. The alternative, that sanukitoids are the relatively fractionated products of lamprophyric magmatism, avoids this unique requirement, and is consistent with the geochemical data presented here and by Perring and Rock (1991). The trace-element enrichment patterns in both lamprophyres and sanukitoid are characteristic of fluid-mediated mantle metasomatism where the mobility of HFSE is greatly inhibited compared with that of REE (LREE>HREE) and LILE. On mantle-normalized trace-element diagrams (Fig. 5) this is expressed as prominent negative Nb (Ta) and Zr (Hf) anomalies. This explains the diagnostic trends to high and variable La/Nb ratios at low Nb concentrations (Fig. 13b). As with shoshonites, strong enrichments in P, Ba and Sr are also diagnostic. Interestingly, the enrichments in Sr are associated with low concentrations of Y and HREE, resulting in extreme Sr/Y ratios (up to >200). Felsic rocks with such ratios are also associated with extraction of magmas, such as tonalite–trondhjemite–granodiorite (TTG), at very high pressures from garnet-bearing, plagioclase-poor (or free), mafic sources. In the case of the EGST lamprophyres series and the sanukitoids, there are several reasons that the high Sr/Y ratios are probably the result of multiple factors, perhaps in addition to garnet retention in the source. First, metasomatism itself enriches the mantle lithosphere, generating a source with elevated Sr/Y.

Such enrichments are also evident in the syenitic rock of the EGST, themselves lithospheric melts (Smithies and Champion, 1999). Second, the peridotitic source (rather than simply high pressures) rules out significant plagioclase in the source, meaning that Sr acts as a strongly incompatible element. Third, the abundance of hornblende indicates a hydrous primary magma. This has the effect of further retarding plagioclase crystallization (enhancing Sr concentration in the melt), while enhancing hornblende fractionation which removes Y and HREE (Dy > Yb) from the melt. This process manifests itself in decreasing Dy/Yb ratios and increasing Sr/Y ratios with increasing silica, without systematic development of negative Sr or Eu anomalies.

Taylor et al. (1994) noted that lamprophyres from the EGST showed a wide range in K_2O/Na_2O ratios and attributed much of the scatter, and particularly the large proportion of more sodic compositions, to post-emplacement hydrothermal alteration. Our dataset provides no evidence that the more sodic rocks have undergone more extensive alteration. There is no correlation between K_2O/Na_2O ratios and alteration-sensitive ratios such as Th/U, which remain close to mantle values of ~4 (Sun and McDonough, 1989) for most data (Fig. 16a). In addition, LOI, if anything, shows a weak positive correlation with K_2O/Na_2O ratios, suggesting that it is the more potassic rocks, if any, that reflect greater alteration (Fig. 16b). An intriguing alternative hypothesis for the generally sodic nature of the EGST calc-alkaline lamprophyres is that the component that enriched their peridotitic source was itself very sodic, containing little of the high-K 'continental' material that contributes to subduction-enriched source regions that produce lamprophyric rocks and shoshonites in post-Archean successions.

Comparisons with regional granitic rocks

Champion and Sheraton (1997) and Cassidy et al. (2002) divided the granitic rocks of the Yilgarn Craton into four main groups. These include high-Ca granites, which are broadly equivalent to the Archean TTG series, low-Ca granites, which were typically derived from more evolved, enriched, sources than high-Ca granites, high HFSE granites, which are fractionated granites transitional in some respects to A-type magmas and contain a significant tholeiitic parental magma component, and Mafic granites. The Mafic granites are typically LILE- and LREE-enriched dioritic to granodioritic rocks forming small intrusions scattered throughout the EGST (Fig. 17), primarily along major structures. The unenriched volcanic rocks primarily have compositions equivalent to the high- and low-Ca granites, but locally also include rocks with compositions such as those of the HFSE granites. Such HFSE-rich 'unenriched' felsic volcanic rocks, for example, dominate the Melita, Teutonic Bore and Spring Well Formations in the western Kurnalpi and northern Kalgoorlie Terranes.

Apart from the sanukitoid dykes described here, sanukitoid intrusions elsewhere in the EGST form the dominant component of the Mafic granite group. More than 75% of the Mafic granites clearly conform to the compositional criteria used here to uniquely identify EGST enriched series (Fig. 18). Approximately 20% of high-Ca granites also fall into the field for enriched felsic volcanic rocks, potentially suggesting that this group incorporates rocks from a range of different origins.

The crystallization ages of the Mafic granites also lie mostly between 2.67 and 2.65 Ga (Witt et al., 2013), significantly overlapping the crystallization ages of other members of the enriched series. Thus, we suggest that most of the units comprising the BFG and scattered eruptive and subvolcanic intrusions elsewhere throughout the EGST, are the eruptive or subvolcanic equivalents of the dominant component of the 'Mafic' group of Yilgarn Craton granites, which are sanukitoids.

A relationship with gold mineralization?

A strong spatial and temporal relationship has empirically been noted in the EGST and elsewhere, first between lamprophyres and gold mineralization and more recently between sanukitoid and gold mineralization (e.g. Rock and Groves, 1988a,b; Rock et al., 1989; Champion and Sheraton, 1997; Halley, 2007; Fayol and Jébrak, 2017; Witt, 2016; Witt et al., 2013, 2015). In the EGST, the age range for the main period of lamprophyre–sanukitoid magmatism (including the BFG and other enriched felsic volcanic and subvolcanic rocks) is c. 2.68 to 2.64 Ga. Taking into account only ages determined using U–Pb in zircon, the age brackets on gold mineralization are c. 2.66 to 2.64 Ga (e.g. Mueller et al., 2008; Vielreicher et al., 2015, 2016).

In a comprehensive investigation and assessment of potential gold mineralization targeting criteria for the Yilgarn Craton, Witt et al. (2013, 2015) demonstrated statistically a 'real and significant geological relationship' between significant gold mineralization and the Mafic granites. These authors noted that the Mafic granites and lamprophyres likely all derive from a metasomatized lithospheric mantle (e.g. Rock and Groves, 1988a,b; Champion and Sheraton, 1997; Cassidy et al., 2002), and stated that 'one of the strongest (statistical) associations with gold was achieved by combining all intrusions with a metasomatized mantle source component (mainly Mafic granites and lamprophyres) in the combined Kalgoorlie and Kurnalpi Terranes, which resulted in capture of 54.1% of the gold endowment and 19.4% of deposits in the 1000 m buffer (of the intrusions)'. In this respect, our findings that lamprophyres, sanukitoids and Mafic granites in fact form a comagmatic and cogenetic series is not surprising. The suggestion that at least 75% of the igneous components (including porphyritic intrusions) of the BFG are the extrusive or subvolcanic equivalents of sanukitoids, is surprising, and would further significantly strengthen the statistical relationship between enriched series magmatism and gold mineralization in the EGST.

The relationship between gold mineralization and lamprophyre–sanukitoid magmatism is frequently viewed as coincidental, both relying on a common structural control (e.g. Goldfarb et al., 2005), i.e. both using the same translithospheric pathways. Clearly, the very presence of lamprophyre–sanukitoid magmatism indicates proximity to a translithospheric fluid pathway tapping metasomatized sources that were also potentially volatile rich and 'fertile' with respect to gold, and perhaps other metals such as

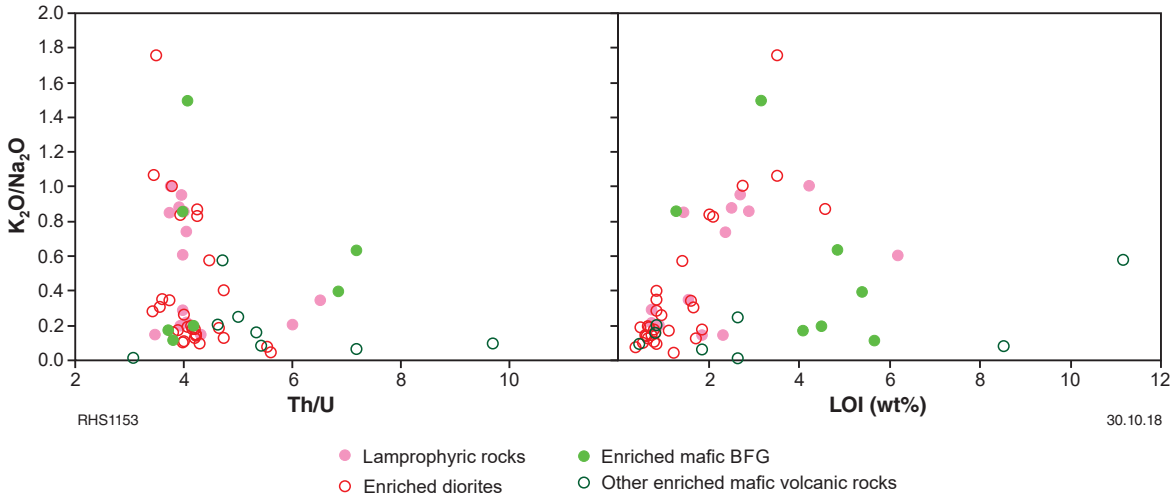

Figure 16. Variation of K_2O/Na_2O with both Th/U and LOI for lamprophyric rocks, enriched diorites, enriched mafic BFG rocks and regional equivalents

copper. The same pathway likely also had the capacity to channel vast volumes of both hydrothermal fluids derived from the volatile lithospheric mantle source as well as crustal metamorphic fluids that were convected into the system during periods of contemporaneous magmatism (e.g. Hronsky et al., 2012).

A more direct genetic association between gold and lamprophyre–sanukitoid magmatism has also been suggested both for the EGST and in other Archean terranes (e.g. Beakhouse et al., 1999; Halley, 2007; Fayol and Jébrak, 2017; Witt, 2016). While an intrinsically high gold content in any of these magmas has never been proven (e.g. Taylor et al., 1994), this might not significantly diminish a critical role for lamprophyre–sanukitoid magmatism in a wider gold mineral system.

If a genetic relationship exists, then the volatile-rich nature of the magmatism is almost certainly extremely important. The frequent presence of calc-alkaline lamprophyre, as dykes, indicates that prevailing stress fields were periodically amenable to small-volume, primitive, mantle-derived magmas ascending rapidly and virtually unmodified over the entire lithospheric column. Crosscutting relationships with each other and with respect to peak-metamorphic assemblages and gold mineralization (e.g. Perring and Rock, 1991; Taylor et al., 1994), and the reasonably long duration throughout which the dykes themselves were emplaced (c. 2.68 to 2.64 Ga), indicates that the required stress fields were repeated or intermittent. If sanukitoids (and thus the Mafic granites) and their even more evolved dacitic and rhyolitic residual magmas are the result of fractionation of more primitive lamprophyre magmas, then local (or regional) stress fields need to have occasionally allowed the ascent of larger volumes of lamprophyre magma. This ascent must either have been arrested, forming a staging chamber (Mafic granites), or slow enough that fractional crystallization modified the lamprophyre magmas into felsic, sanukitoid compositions. Such a process would have released enormous volumes of volatile-rich magmatic fluids, which were likely also relatively oxidized. Irrespective of their initial gold content, these fluids would have had a capacity to scavenge metals along their ascent pathways.

Throughout the EGST, regional variations in the relative abundance of lamprophyre dykes, or dyke swarms (e.g. Taylor et al., 1994), sanukitoid plutons (Mafic granites), sanukitoid dykes, and sanukitoid-like (enriched) volcanic rocks might reflect spatial or temporal variations in local or regional stress fields and in levels of exposure. Exposed Mafic granite intrusions, for example, reflect moderately deep crustal levels whereas volcanic sanukitoids obviously reflect the uppermost levels.

The BFG itself collectively represents perhaps the largest exposed volume of sanukitoid magma in the EGST. If the suggestion that this derived from a mafic lamprophyric magma is correct then the BFG relates directly to a significantly greater volume of cumulate material and coarse-grained, primitive sanukitoid (i.e. large Mafic granite intrusions) at depth beneath the Kalgoorlie–Kambalda region. These intrusions reflect the cumulate products of a significantly greater volume of volatile-rich lamprophyric magma, and the genetic pathway between these and the BFG involved exsolution of an extraordinary volume of volatile-rich fluids. Given the wide compositional variation between individual groups of spatially related lamprophyric rocks and sanukitoids (e.g. Figs 8, 9), this mass of enriched magma was likely a composite intrusion formed from a large number of individual magma batches, perhaps over a wide period of time. The extraordinary gold endowment of the areas within and peripheral to the BFG might indicate that these very shallow systems reflect the most favourable crustal level in terms of (magmatic) gold mineralization. Alternatively, the extraordinary volume of lamprophyre–sanukitoid magmatism in that region might reflect either an extremely efficient translithospheric fluid pathway or a particularly volatile-rich and fertile lithospheric mantle source, or a combination of all these factors. Regardless, the identification of ‘enriched’ signatures in EGST felsic volcanic and subvolcanic rocks is probably a very encouraging pointer to regions of enhanced gold-mineralization potential.

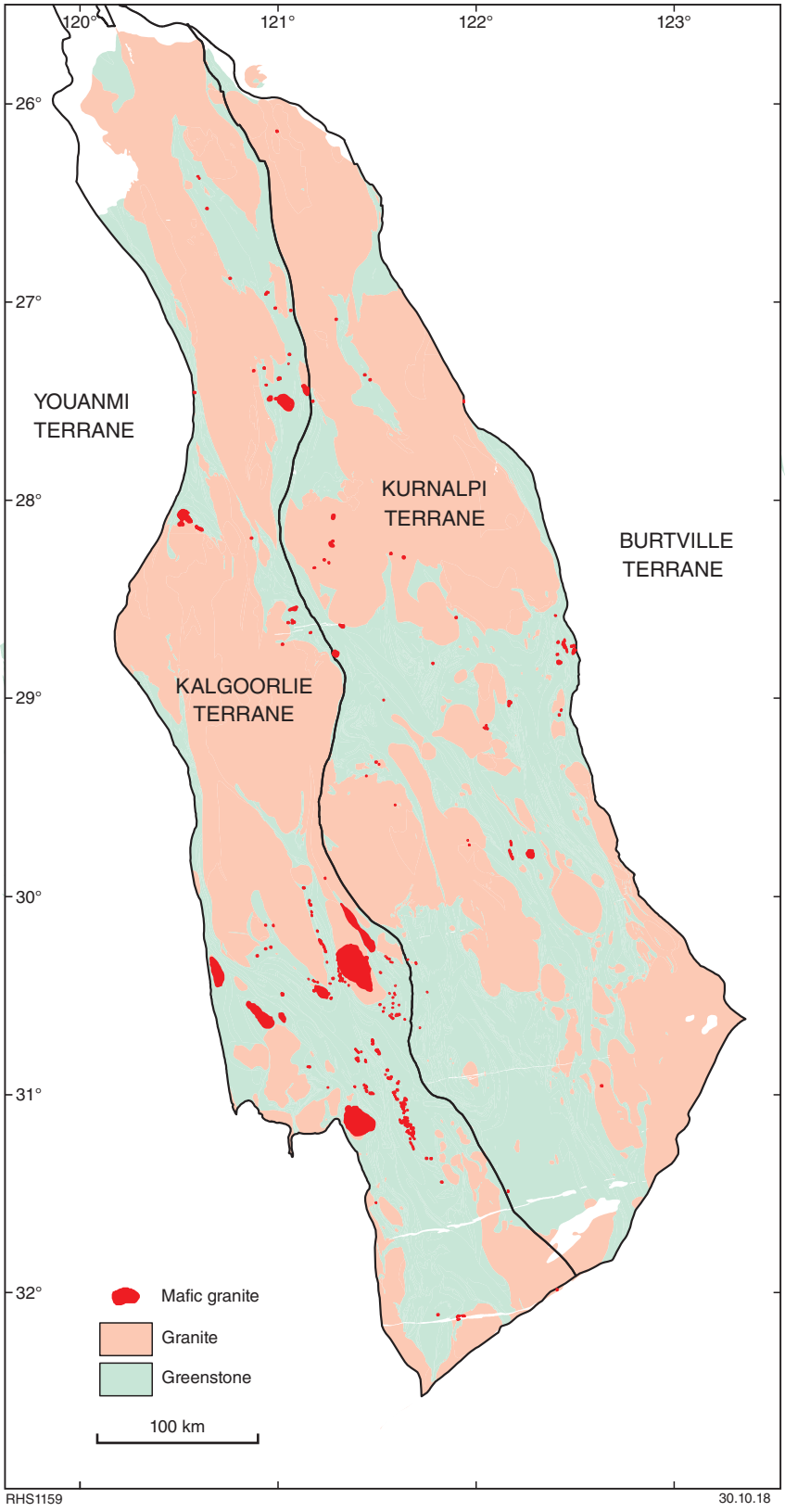

Figure 17. Distribution of Mafic granites throughout the Kalgoorlie and Kurnalpi Terranes of the EGST (modified after Witt et al., 2013)

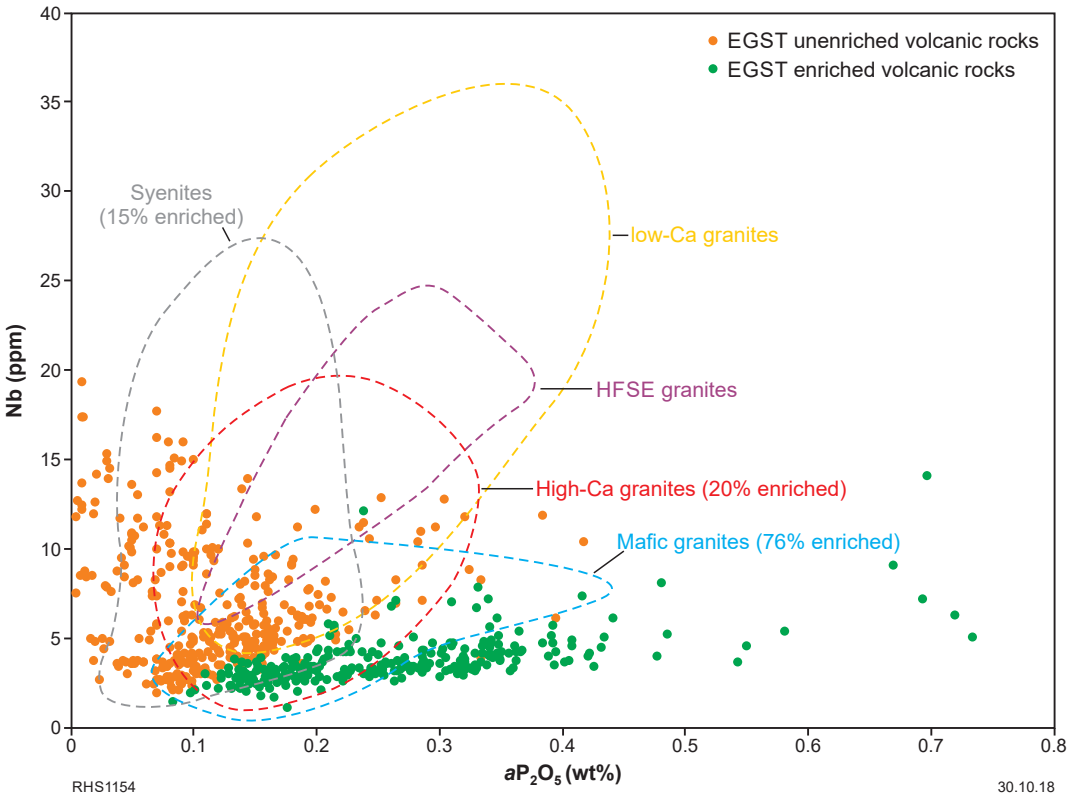

Figure 18. Variation in Nb with aP_2O_5 comparing the enriched and unenriched felsic rocks (volcanic and subvolcanic) with Yilgarn Craton granitic rock groups described by Champion and Sheraton (1997) and Cassidy et al. (2002). Also indicated for some granitic rock groups are the proportions of samples that fall within the field for 'enriched' rocks as defined here. In the case of the Mafic granite group, 76% overlap the enriched volcanic rock field defined by the spread of green circles

Conclusions

An empirical relationship between gold mineralization and compositionally specialized lamprophyric and sanukitoid magmas has long been recognized, and more recently statistically verified. In the EGST, trace element-enriched dioritic intrusions, compositionally and mineralogically transitional with lamprophyric dykes have been recognized, and this study directly identifies these dioritic rocks as sanukitoids. Moreover, this study supports the suggestion (Perring and Rock, 1991) that the diorites (sanukitoids) are directly related to lamprophyric magmas through a liquid line of descent involving hornblende fractionation, rather than through direct extraction from lithospheric mantle. Together, lamprophyres and sanukitoids define a distinct low Nb, high P_2O_5 magmatic association. More than 75% of Mafic granites (one of the four main granitic rock groups of the Yilgarn Craton) fall within this association. Most significantly, more than 75% of the igneous rocks forming the BFG also fall within this distinct 'enriched' association, i.e. most BFG rocks are volcanic equivalents of evolved sanukitoids (or Mafic granites). Smaller occurrences of similar felsic volcanic rocks lie throughout the EGST but are not as abundant or regionally extensive as 'unenriched' felsic volcanic and subvolcanic rocks.

The origins of the enriched magmas can be traced back to a metasomatized lithospheric source and so the occurrence of such magmas indicates proximity to a translithospheric structure. The significance of a genetic link between lamprophyric magmas and sanukitoids, and further to more evolved dacitic compositions of the BFG, is that protracted fractionation of wet hornblende-bearing lamprophyric magma involves exsolving enormous volumes of relatively oxidized fluids, which are subsequently channelled along translithospheric pathways. Even if such fluids are not initially intrinsically gold rich, they likely scavenge a significant metal cargo as they ascend through the crustal greenstone sequences. Additionally, even if such a process seldom produced primary gold mineralization, it may have represented a critical enrichment process along long-lived fluid pathways. The extraordinary gold endowment of the areas within and peripheral to the BFG might indicate that these very shallow systems reflect the most favourable crustal level in terms of (magmatic) gold enrichment. Alternatively, the extraordinary volume of lamprophyre–sanukitoid magmatism in that region might reflect either an extremely efficient translithospheric fluid pathway or a particularly volatile-rich and fertile lithospheric mantle source, or a combination of all these factors.

The regional distribution of Mafic granites, and the composition of felsic volcanic and subvolcanic units in terms of 'enriched' or 'unenriched' characteristics described here remain poorly established.

Acknowledgements

We thank Northern Star Resources Ltd for permission to use images shown in Figure 14. Alicia Verbeeten and David Nixon are thanked for numerous stimulating conversations that contributed to this study.

References

Baggott, MS 2006, A refined model for the magmatic, tectonometamorphic, and hydrothermal evolution of the Leonora District, Eastern Goldfields Province, Yilgarn Craton, Western Australia: The University of Western Australia, Perth, Western Australia, 267p (unpublished).

Barnes, SJ, and Van Kranendonk, MJ 2014, Archean andesites in the east Yilgarn Craton, Australia: Products of plume-crust interaction?: Lithosphere, v. 6, p. 80–92.

Barnes, SJ, Van Kranendonk, MJ and Sonntag, I 2012, Geochemistry and tectonic setting of basalts from the Eastern Goldfields Superterrane: Australian Journal of Earth Sciences, v. 59, p. 707–735.

Beakhouse, GP, Heaman, LM and Creaser, RA 1999 Geochemical and U–Pb zircon geochronological constraints on the development of a Late Archean greenstone belt at Birch Lake, Superior Province, Canada: Precambrian Research, v. 97, p.77–97.

Brown, SJA, Barley, ME, Krapež, B and Cas, RAF 2002, The Late Archaean Melita Complex, Eastern Goldfields, Western Australia: shallow submarine bimodal volcanism in a rifted arc environment: Journal of Volcanology and Geothermal Research, v. 115, no. 3–4, p. 303–327.

Cassidy, KF, Champion, DC, McNaughton, NJ, Fletcher, IR, Whitaker, AJ, Basttakova, IV and Budd, AR 2002, Characterisation and metallogenic significance of Archean granitoids of the Yilgarn Craton, Western Australia: Minerals and Energy Research Institute of Western Australia (MERIWA), Report 222, 514p.

Corriveau, L, Montreuil, J-F and Potter, EG 2016, Alteration facies linkages among iron oxide copper-gold, iron oxide-apatite, and affiliated deposits in the Great Bear Magmatic zone, Northwest Territories, Canada: Economic Geology, v. 111, p. 2045–2072.

Champion, DC and Sheraton, JW 1997, Geochemistry and Nd isotope systematics of Archaean granites of the Eastern Goldfields, Yilgarn Craton, Australia: implications for crustal growth processes: Precambrian Research, v. 83, p. 109–132.

Czarnota, K, Champion, DC, Goscombe, B, Blewett, RS, Cassidy, KF, Henson, PA and Groenewald, PB 2010 Geodynamics of the eastern Yilgarn Craton: Precambrian Research, v. 183, no. 2, p. 175–202.

Fayol, N and Jébrak, M 2017, Archean Sanukitoid Gold Porphyry Deposits: A New Understanding and Genetic Model from the Lac Bachelor Gold Deposit, Abitibi, Canada: Economic Geology, v. 112, p. 1913–1936.

Fletcher, IR, Dunphy, JM, Cassidy, KF and Champion, DC 2001, Compilation of SHRIMP U-Pb geochronological data, Yilgarn Craton, Western Australia, 2000–2001: Geoscience Australia, Geoscience Australia Record 2001/47, 111p.

Fowler, MB and Henney, PJ 1996, Mixed Caledonian appinite magmas: implications for lamprophyre fractionation and high Ba–Sr granite genesis: Contributions to Mineralogy and Petrology, v. 126, p. 199–215.

Goldfarb, RJ, Baker, T, Dubé, B, Groves, DI, Hart, CJR, Robert, F and Gosselin, P 2005, Distribution, productivity, character, and genesis of gold deposits in metamorphic terranes, *in* Economic Geology One Hundredth Anniversary volume *edited by* JW Hedenquist, JFH Thompson, RJ, Goldfarb and JP Richards: Society of Economic Geologists, p. 407–450.

Halley, S 2007, Mineral mapping – how it can help us explore in the Yilgarn Craton, *in* Proceedings of Geoconferences (WA) Inc Kalgoorlie '07 Conference *edited by* FP Bierlein and CM Knox-Robinson, September, 2007: Geoscience Australia, Record 2007/14, p. 143–144.

Hronsky, JMA, Groves, DI, Loucks, RR and Begg, GC 2012, A unified model for gold mineralisation in accretionary orogens and implications for regional-scale exploration targeting methods: Mineralium Deposita, v. 47, p. 339–358.

Kositcin, N, Brown, SJA, Barley, ME, Krapež, B, Cassidy, KF and Champion, DC 2008, SHRIMP U–Pb zircon age constraints on the Late Archaean tectonostratigraphic architecture of the Eastern Goldfields Superterrane, Yilgarn Craton, Western Australia: Precambrian Research, v. 161, p. 5–33.

Lorand, JP, Bodinier, JL, Dupuy, C, and Dostal, 1989, Abundance and distribution of gold in the orogenic-type spinel peridotites from Ariege (north-eastern Pyrenees, France): Geochimica et Cosmochimica Acta, v. 53, p. 3085–3090.

Martin, H, Smithies, RH, Rapp, R, Moyen, J-F and Champion, D 2005, An overview of adakite, tonalite-trondhjemite-granodiorite (TTG), and sanukitoid: relationships and some implications for crustal evolution: Lithos, v. 79, p. 1–24.

Morris, PA 1993, Archaean mafic and ultramafic volcanic rocks, Menzies to Norseman, Western Australia: Geological Survey of Western Australia, Report 36, 107p.

Morris, PA 1998, Archaean felsic volcanism in parts of the Eastern Goldfields region, Western Australia: Geological Survey of Western Australia, Report 55, 80p.

Morris, PA and Witt, WK 1997, Geochemistry and tectonic setting of two contrasting Archaean felsic volcanic associations in the Eastern Goldfields, Western Australia: Precambrian Research, v. 83, p. 83–107.

Morris, PA and Kirkland, CL 2014, Melting of a subduction-modified mantle source: A case study from the Archean Marda Volcanic Complex, central Yilgarn Craton, Western Australia: Lithos, v. 190–191, p. 403–419.

Mueller, AG, Hall, GC, Nemchin, AA, Stein, HJ, Creaser, RA and Mason, DR 2008, Archean high-Mg monzodiorite-syenite, epidote skarn, and biotite-sericite gold lodes in the Granny Smith-Wallaby district, Australia: U-Pb and Re-Os chronology of two intrusion-related systems: Mineralium Deposita, v. 43, p. 337–362.

Nelson, DR 1995a, 112159: porphyritic dacite, Royal Arthur; Geochronology Record 488: Geological Survey of Western Australia, 5p.

Nelson, DR 1995b, 112110: felsic volcanic rock, Nelson's Fleet; Geochronology Record 526: Geological Survey of Western Australia, 4p.

Nelson, DR 1997a, 118953: porphyritic rhyolite, Spring Well South; Geochronology Record 448: Geological Survey of Western Australia, 4p.

Nelson, DR 1996, 104958: metadacite, Ballarat – Last Chance; Geochronology Record 20: Geological Survey of Western Australia, 4p.

Nelson, DR 1997b, Evolution of the Archaean granite-greenstone terranes of the Eastern Goldfields, Western Australia: SHRIMP U-Pb zircon constraints: Precambrian Research, v. 83, p. 57–81.

Perring, CS, Barley, ME, Cassidy, KF, Groves, DI, McNaughton, NJ, Rock, NMS, Bettenay, LF, Golding, SD and Hallberg, JA 1989, The association of linear orogenic belts, mantle-crustal magmatism, and Archean gold mineralization in the Eastern Yilgarn Block of Western Australia, *in* The Geology of Gold Deposits: The Perspective in 1988 *edited by* RR Keays, WRH Ramsay, and DI Groves: Economic Geology, Monograph 6, p. 571–584.

Perring, CS, and Rock, NMS 1991, Relationships between acidic (dacitic) and primitive (lamprophyric) magmas in late Archaean composite dykes: Precambrian Research, v. 52, p. 245–273.

Perring, CS and McNaughton, NJ 1992, The relationship between Archaean gold mineralization and spatially associated minor intrusions in the Kambalda and Norseman gold camps, Western Australia: lead isotopic evidence: Mineralium Deposita, v. 27, p. 10–22.

Perring, CS, Rock, NMS, Golding, SD, and Roberts, DE 1989, Criteria for the recognition of metamorphosed or altered lamprophyres: a case study from the Archaean of Kambalda, Western Australia: Precambrian Research, v. 43, p. 215–237.

Rock, NMS and Groves, DI 1988a, Can lamprophyres resolve the genetic controversy over mesothermal gold deposits?: Geology, v. 16, p. 538–541.

Rock, NMS and Groves, DI 1988b, Do lamprophyres carry gold as well as diamonds?: Nature, v. 332, p. 253–255.

Rock, NMS, Groves, DI, Perring, CS and Golding, SD 1989, Gold, lamprophyres, and porphyries: What does their association mean?: Economic Geology, Monograph 6, p. 609–625.

Shirey, SB and Hanson, GN, 1984, Mantle-derived Archaean monzodiorites and trachyandesites: Nature, v. 310, p. 222–224.

Smithies, RH and Champion, DC 1999, Late Archaean felsic alkaline igneous rocks in the Eastern Goldfields, Yilgarn Craton, Western Australia: a result of lower crustal delamination?: Journal of the Geological Society of London, v. 156, p. 561–576.

Smithies, RH and Champion DC 2000, The Archaean High-Mg Diorite Suite: Links to Tonalite-Trondhjemite-Granodiorite Magmatism and Implications for Early Archaean Crustal Growth: Journal of Petrology, v. 41, p, 1653–1671.

Stanley, CR and Lawie, D 2007, Average relative error in geochemical determinations: clarification, calculation and a plea for consistency: Exploration and Mining Geology, vol. 16, no. 3–4, p. 265–274.

Stern, RA, Hanson, GN, and Shirey, SB 1989, Petrogenenesis of mantle-derived, LILE enriched Archean monzodiorites and trachyandesites (sanukitoids) in southwestern Superior Province: Canadian Journal of Earth Sciences, v. 26, p. 1688–1712.

Sun, SS and McDonough, WF 1989, Chemical and isotopic systematics of oceanic basalts: implication for mantle composition and processes: Geological Society of London, Special Publications, v. 42, p. 313–345.

Taylor, WR, Rock, NMS, Groves, DI, Perring, CS and Golding, SD 1994, Geochemistry of Archean shoshonitic lamprophyres from the Yilgarn Block, Western Australia: Au abundance and association with gold mineralization: Applied Geochemistry, v. 9, p. 197–222.

Tripp, GI 2013, Stratigraphy and structure in the Neoarchaean of the Kalgoorlie district, Australia: critical controls on greenstone-hosted gold deposits: James Cook University, Townsville, PhD thesis, 773p. (unpublished).

Vielreicher, NM, Groves, DI, McNaughton, N, and Fletcher, I 2015, The timing of gold mineralization across the eastern Yilgarn Craton using U–Pb geochronology of hydrothermal phosphate minerals: Mineral Deposita, v. 50, p. 391–428

Vielreicher, NM, Groves, DI, and McNaughton NJ 2016, The giant Kalgoorlie Gold Field revisited: Geoscience Frontiers, v. 7, p. 359–374.

Wingate, MTD, Kirkland, CL, Bodorkos, S and Hall, CH 2010, 179684: metarhyolite, Buldania Rocks; Geochronology Record 879: Geological Survey of Western Australia, 4p.

Witt, WK 2016, Deposit-scale targeting for gold in the Yilgarn Craton: Part 3 of the Yilgarn Gold Exploration Targeting Atlas: Geological Survey of Western Australia, Report 158, 182p.

Witt, WK, Ford, A, Hanrahan, B, and Mamuse, A, 2013, Regional-scale targeting for gold in the Yilgarn Craton: Part 1 of the Yilgarn Gold Exploration Targeting Atlas: Geological Survey of Western Australia, Report 125, 130p.

Witt, WK, Ford, A, and Hanrahan, B 2015, District-scale targeting for gold in the Yilgarn Craton: Part 2 of the Yilgarn Gold Exploration Targeting Atlas: Geological Survey of Western Australia, Report 132, 276p.

RECORD 2018/15

This Record is published in digital format (PDF) and is available as a free download from the DMIRS website at <www.dmp.wa.gov.au/GSWApublications>.

Further details of geological products produced by the Geological Survey of Western Australia can be obtained by contacting:

Information Centre
Department of Mines, Industry Regulation and Safety
100 Plain Street
EAST PERTH WESTERN AUSTRALIA 6004
Phone: +61 8 9222 3459 Fax: +61 8 9222 3444
www.dmp.wa.gov.au/GSWApublications

A NEW LOOK AT LAMPROPHYRES AND SANUKITOIDS, AND THEIR RELATIONSHIP TO THE BLACK FLAG GROUP AND GOLD PROSPECTIVITY

Smithies et al.